

To the Editor of the International Journal “Science of the Total Environment”

Dear Editor,

please find attached the manuscript entitled: “The environmental impact of air pollution on the built Heritage of Historic Cairo (Egypt)” by Rovella et al., submitted for publication in Science of the Total Environment.

We declare that the manuscript is not under consideration for publication and has not been published elsewhere.

The work was focused on the minero-petrographic and geochemical characterization of black crusts, in terms of heavy metals and carbonaceous fraction, taken from some selected monuments of Historic Cairo. Complementary analytical methods have been applied to investigate the correlation between black crusts and the air pollution of the city, identifying the main pollutant sources and their impact on the state of conservation of the studied sites.

The contents of this manuscript could appeal to the broad readership of the journal because of the strong interdisciplinary nature of the argument and its conformity with the topics dealt with, based on the total environment and in particular, on the interactions between atmosphere, lithosphere and anthroposphere.

We are looking forward to hearing from you. Thank you for your consideration.

Yours sincerely,

Valeria Comite (on behalf of all authors)

Corresponding author’s complete contact details:

Dr. Valeria Comite, Ph.D.

Dipartimento di Chimica – Università degli Studi di Milano

Via Golgi 19, 20133 Milano, Italy.

E-mail: [valeria.comite@unimi.it](mailto:valeria.comite@unimi.it)

Phone: +390250314246

Category of paper: Original Paper

Number of figures that will be printed in color in the printed issue: NONE

Conflicts of interest: NONE

## The environmental impact of air pollution on the built Heritage of Historic Cairo (Egypt)

Natalia Rovella<sup>a</sup>, Nevin Aly<sup>b</sup>, Valeria Comite<sup>c\*</sup>, Luciana Randazzo<sup>a</sup>, Paola Fermo<sup>c</sup>, Donatella Barca<sup>a</sup>, Monica Alvarez de Buergo<sup>d</sup>, Mauro Francesco La Russa<sup>a</sup>

<sup>a</sup> Department of Biology, Ecology and Earth Sciences (DiBEST), University of Calabria, 87036 Arcavacata di Rende, CS, Italy

[natalia.rovella@unical.it](mailto:natalia.rovella@unical.it); [luciana.randazzo@unical.it](mailto:luciana.randazzo@unical.it); [donatella.barca@unical.it](mailto:donatella.barca@unical.it); [mlarussa@unical.it](mailto:mlarussa@unical.it)

<sup>b</sup> Department of Science and Engineering Mathematics, Faculty of Petroleum and Mining Engineering, Suez University, 43512 Suez, Egypt

[Nevin.Aly@suezuniv.edu.eg](mailto:Nevin.Aly@suezuniv.edu.eg)

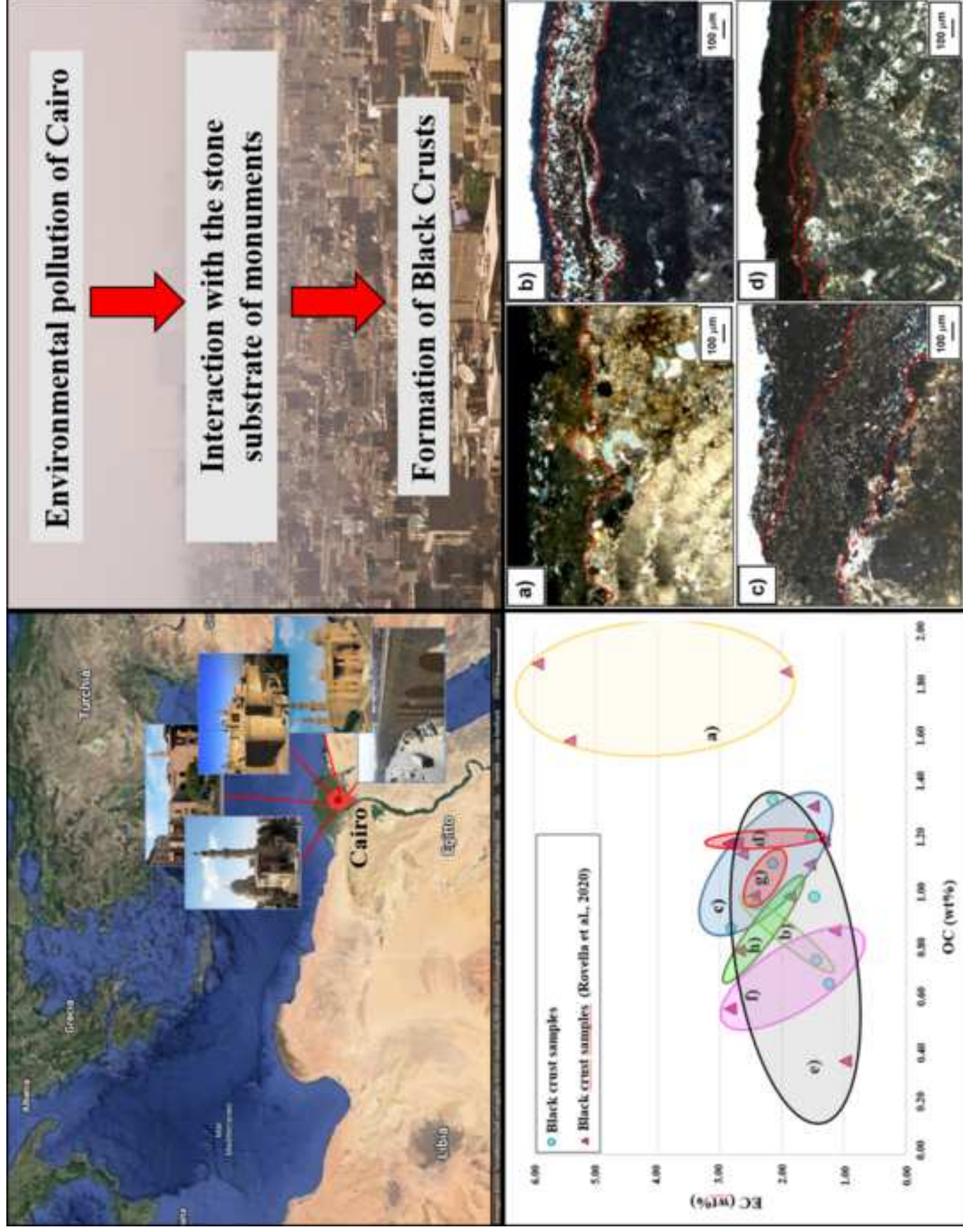
<sup>c</sup> Department of Chemistry, University of Milan, Via Golgi 19, 20133 Milan, Italy

[valeria.comite@unimi.it](mailto:valeria.comite@unimi.it); [paola.fermo@unimi.it](mailto:paola.fermo@unimi.it)

<sup>d</sup> Geosciences Institute IGEO (CSIC-UCM), Doctor Severo Ochoa 7, 28040 Madrid, Spain

[alvarezm@geo.ucm.es](mailto:alvarezm@geo.ucm.es)

\*corresponding author: [valeria.comite@unimi.it](mailto:valeria.comite@unimi.it)



**\*Highlights (for review : 3 to 5 bullet points (maximum 85 characters including spaces per bullet point)**

**Highlights:**

- Black crusts from Cairo have been analyzed by several techniques
- The effect of urban air pollution on the monuments of Cairo have been investigated
- The methodology allowed identification of pollution sources in the black crusts

1                   **The environmental impact of air pollution on the built Heritage**  
2   **of Historic Cairo (Egypt)**

3  
4  
5           Natalia Rovella<sup>a</sup>, Nevin Aly<sup>b</sup>, Valeria Comite<sup>c\*</sup>, Luciana Randazzo <sup>a</sup>, Paola Fermo <sup>c</sup>, Donatella  
6   Barca <sup>a</sup>, Monica Alvarez de Buergo <sup>d</sup>, Mauro Francesco La Russa <sup>a</sup>

7  
8  
9           <sup>a</sup> Department of Biology, Ecology and Earth Sciences (DiBEST), University of Calabria, 87036  
10   Arcavacata di Rende, CS, Italy

11   [natalia.rovella@unical.it](mailto:natalia.rovella@unical.it); [luciana.randazzo@unical.it](mailto:luciana.randazzo@unical.it); [donatella.barca@unical.it](mailto:donatella.barca@unical.it);  
12   [mlarussa@unical.it](mailto:mlarussa@unical.it)

13  
14           <sup>b</sup> Department of Science and Engineering Mathematics, Faculty of Petroleum and Mining  
15   Engineering, Suez University, 43512 Suez, Egypt

16   [Nevin.Aly@suezuniv.edu.eg](mailto:Nevin.Aly@suezuniv.edu.eg)

17  
18           <sup>c</sup> Department of Chemistry, University of Milan, Via Golgi 19, 20133 Milan, Italy

19   [valeria.comite@unimi.it](mailto:valeria.comite@unimi.it); [paola.fermo@unimi.it](mailto:paola.fermo@unimi.it)

20  
21           <sup>d</sup> Geosciences Institute IGEO (CSIC-UCM), Doctor Severo Ochoa 7, 28040 Madrid, Spain

22   [alvarezm@geo.ucm.es](mailto:alvarezm@geo.ucm.es)

23  
24           \*corresponding author: [valeria.comite@unimi.it](mailto:valeria.comite@unimi.it)

26

27 **Abstract**

28

29 In the last decades, many researchers investigated the relation between environmental pollution and  
30 the degradation phenomena on the built heritage, because of their rapid increase and growing  
31 harmfulness. Consequently, the identification of the main pollution sources has become essential to  
32 define mitigation actions against degradation and alteration phenomena of the stone materials. In  
33 this way, the present paper is focused on the study of the effect of air pollution on archaeological  
34 buildings in Historic Cairo.

35 A multi-methodological approach was used to obtain information about the chemical composition  
36 of examined black crusts and to clarify their correlation with the air pollution, specifically the heavy  
37 metals and the carbonaceous fraction, their main sources, and their impact on the state of  
38 conservation of the studied sites.

39 All specimens were characterized by polarized optical microscopy (POM), X-Ray Diffraction  
40 (XRD), Electron Probe Micro Analyser coupled with energy dispersive X-ray spectrometry  
41 (EPMA-EDS), laser ablation inductively coupled plasma mass spectrometry (LA-ICP-MS) and  
42 Thermo-gravimetric analysis (TGA).

43 The results indicate a good correlation between the composition of black crusts and the main  
44 pollutant sources in Cairo such as vehicular traffic and industrial activities.

45

46 **Keyword:** air pollution; built cultural heritage; black crust; heavy metals; carbonaceous fraction;  
47 degradation.

48

49

50

## 1. Introduction

52

53 Cairo is the largest city in Egypt and in Africa; here, the air pollution produced many environmental  
54 problems related to aerosol particulate matter and to the high levels mostly of sulphur dioxide and  
55 lead. For this reason, it was listed as one of the most polluted cities in the world (Gurjar et al.,  
56 2010). The air pollution sources in the city are different and include burning of rubbish, vehicle  
57 emissions (~4.5 million cars on the streets of Cairo) and urban industrial activities. The city has 15–  
58 20 million inhabitants and is characterized by high congestion due to a population density of  
59 13107/km<sup>2</sup> (Abbass et al., 2020). Furthermore, the lack of rain helps the accumulation of pollutants.  
60 The entire area of Cairo is severely affected by industrial and urban emissions of metals and  
61 metalloids (Abdel-Latif and Saleh, 2012). For example, only the cement industry releases around  
62 2.4 million tons per year of cement bypass dust into the atmosphere (Alkhdhairi et al., 2018).  
63 Moreover, it was estimated that the high Particulate Matter (PM) concentrations cause around 10 %  
64 of premature deaths in Egypt, where the national cost of air pollution is estimated at \$20.9 million  
65 (Abbass et al., 2020).

66 An important factor that contributes to the air pollution increase is represented by the climatic  
67 conditions (Lowenthal et al., 2014; Alkhdhairi et al., 2018) and the remarkable seasonal  
68 temperature changes; in fact, its climate is classified as hot arid (BWh, according to the Köppen and  
69 Geiger (1936) climate classification).

70 At the same time, Cairo city produces 10,000 Tm of waste daily, often burned illegally. Previous  
71 studies on air pollution and atmospheric aerosols emissions from industrial and urban sites in  
72 Greater Cairo Area (GCA) highlighted how heavy metals represent a relevant and worrying  
73 component (Robaa, 2003; Abu-Allaban et al., 2007, 2009; Zakey et al., 2008; Abdel-Latif and  
74 Saleh, 2012; Shaltout 2013a,b, 2014).

75 Borai and Soliman (2001) demonstrate a direct relationship in Cairo city between the trace metals  
76 (e.g. Pb, Cd, Zn, Ni, Mn, Pb, Zn, and Cu) present in the aerosol PM and the anthropogenic activities  
77 such as vehicular traffic and industries, specifically, ferrous metallurgical work, foundries, lead  
78 smelters, lead batteries, ceramics, glass, bricks, textiles and plastics.

79 In this regard, many lead and copper smelters that heavily pollute the city air are unregistered. This  
80 fact produced a permanent haze over the city with PM reaching over three times the normal levels  
81 (Creighton et al., 1990).

82 In some studies (Khairy et al., 2011; Abdel-Latif and Saleh, 2012), the role of the road dust is  
83 clarified: dust deposits and accumulates on ground surfaces, along roadsides that are contaminated  
84 by heavy metals and organic matter. It does not remain deposited in place for long but is easily re-  
85 suspended back into the atmosphere, where it provides a significant amount of trace elements. The  
86 mentioned reference indicates that road dust within Cairo contains higher concentrations of  
87 elements (Pb, Zn, Cd, As, Sn and V) mainly reflecting the contribution of vehicular traffic and  
88 industrial activities.

89 Pollutants are deposited on the surface of stone materials constituent of the historical buildings.  
90 Indeed, those ones suffer serious deterioration phenomena in Cairo as a result of physical-chemical  
91 and biological effects (El-Tawab et al., 2012), favouring black crust formation, alveolization,  
92 chemical alterations, disaggregation pitting, cracks, erosion (Davidson et al., 2000).

93 Black crusts are one of the most dangerous degradation products in building stones and are closely  
94 connected with environmental pollution, especially the atmospheric one. They are very common on  
95 the carbonate substrates such limestones. This lithotype is widely used for the construction of  
96 historical monuments in the whole Mediterranean area thanks to its workability, durability and  
97 aesthetic features; nevertheless it is frequently affected by degradation phenomena (Fitzner et al.,  
98 2002; La Russa et al., 2013a; Ricca et al., 2019) firstly black crusts.

99 They are formed through sulphating processes of the stone surface where calcium carbonate  
100 (CaCO<sub>3</sub>), which is the main constituent of limestone, is transformed into gypsum CaSO<sub>4</sub>\*2H<sub>2</sub>O



101 (Whalley et al., 1992; Comite et al., 2012, 2019, 2020a,b; Rovella et al., 2020). Metals and metal  
102 oxides, present in the atmosphere, catalyse the sulphating reaction (Fermo et al., 2020). This  
103 process affects mainly stone materials having carbonate nature (for example limestone, marble,  
104 lime mortar). In addition, during the crust formation, particulate matter, which contains mainly  
105 amorphous carbon and several heavy metals, can be embedded into the gypsum, providing its  
106 characteristic black colour (La Russa et al., 2018) and altering the aesthetic appearance of the  
107 monuments. For instance, the old structures in Cairo, originally of a whitish colour and some even  
108 striped with the “ablaq” style (in some instances it is hard to spot the stripes due to the amount of  
109 dust covering the surface) are now completely blackened (Orphy and Hamid, 2004). Moreover,  
110 black crusts threaten the conservation of the stone surfaces: hard crusts, usually firmly attached to  
111 the stone are very hard to remove and can weaken the surface on which they develop.

112 For all these reasons the attention of the scientific world is steadily increasing on the effect of air  
113 pollution on archaeological buildings in Cairo and, consequently on the relative degradation  
114 products, (Fitzner et al., 2002; Khallaf, 2011; Kukela and Seglins, 2011; Abdelmegeed et al., 2019).

115 The present research was conceived in this context and deals with the relation between air pollution  
116 and the historical building in Cairo.

117 The study areas are located in the historic Cairo (Fig. 1S available in *Supplementary material*) and  
118 includes the outer walls of Salah El-Din citadel, the Magra El-Oyoun wall, and monuments of the  
119 Northern Mamluk cemetery such as the Mosque of the Sultan Faraj ibn Barquq, the Qaitbay  
120 Mosque and the tomb of Qansuh Al-Ghuri. They were selected for historical-artistic relevance,  
121 location in the urban context characterized by different prevailing pollution sources and building  
122 stone materials (i.e., limestone).A complementary analytical approach was applied to gain  
123 information on the chemical composition of the collected black crusts and define a correlation  
124 between the air pollution, especially the heavy metals contribution and the carbonaceous fraction,  
125 and their main sources , as well as to study the conservation state of the investigated sites.

126 The samples were characterized by polarized optical microscopy (POM), X-Ray Diffraction (XRD),  
127 Electron Probe Micro Analyser coupled with energy dispersive X-ray spectrometry (EPMA-EDS),  
128 laser ablation inductively coupled plasma mass spectrometry (LA-ICP-MS) and Thermo-  
129 gravimetric analysis (TGA).

130

## 131 **2. Materials and Methods**

132 The limestones used for the construction of the historical stone monuments in Cairo come from  
133 local middle and late Eocene outcrops (47.8- 33.9 million years ago) located in Mokattam, Helwan  
134 and Giza areas (El-Nahhas et al., 1990; Ahmed et al., 2006; Park and Shin, 2009; Aly et al., 2015,  
135 2020). These materials are still being used for stone replacement or rebuilding works in monuments  
136 preservation practice as well as for modern buildings.

137 All the monuments underwent various rebuilding interventions over time and there is not very  
138 reliable information about them. Regarding restoration in modern epoch, it is known that several  
139 interventions were carried out in the 19<sup>th</sup> century, 1990s and early 2000s.

140 Samples consist of black crust and stone substrate, were taken from some  
141 portions located on vertical surfaces of the selected monuments, seriously affected by degradation  
142 phenomena and exposed to high rates of environmental pollution (Table 1).

143 A complete characterization of stone substrate and black crust associated was carried out, applying  
144 different analytical techniques aimed to determining the stationary and mobile combustion sources,  
145 major responsible for the blackening and soiling encountered.

146 POM analyses were performed on polished thin sections by using a Zeiss Axiolab associated with  
147 AxioCam MR for digital image acquisition. This technique is aimed to characterize both substrate  
148 and black crusts and to investigate the substrate/black crust interface determining minero-  
149 petrographic features and evaluating the degradation degree of each sample.

150 XRD analysis was carried out to identify the mineralogical phases constituting the black crusts  
151 sampled. Measurements were performed using a Siemens D5000 diffractometer and spectra were  
152 taken in the range  $5^{\circ}$ – $65^{\circ}$   $2\Theta$ , using a step-size of  $0.02^{\circ}$   $2\Theta$  and a step-time of 2 s/step.

153 Samples were carefully prepared by separating the limestone substrate from the black crust and  
154 pulverized them in an agate mortar.

155 An EPMA - JEOL - JXA 8230 —coupled with an EDS spectrometer - JEOL EX-94310FaLIQ -  
156 Silicon drift type— was used in order to observe the micro-morphology and analyse the  
157 composition in terms of major chemical elements. The EDS analyses were carried out according to  
158 the following operating conditions: 15 keV HV; 10 nA probe current; 11mm working distance;  $40^{\circ}$   
159 take off; and 30 seconds live time. Before measuring, samples were graphite (ultra-pure graphite)  
160 sputtered to facilitate the electron conductivity by generating a  $\pm 5$  nm thick film, applied by Sputter  
161 - Carbon Coater QUORUM Q150T-ES, 70 A pulse current and 2.5 sec pulse time).

162 Chemical analyses of the black crusts, as well as of the substrates, in terms of trace elements were  
163 performed by LA-ICP-MS. This method can analyse a great number of chemical elements with a  
164 spot resolution of approximately 40–50  $\mu\text{m}$ , which also allows the determination of compositional  
165 variations at a micrometric scale. Analyses were carried out using an Elan DRCe instrument (Perkin  
166 Elmer/SCIEX), connected to a New Wave UP213 solid-state Nd-YAG laser probe ( $\lambda=213$  nm).

167 Samples were ablated by a laser beam in a cell following the method tested by Gunther and  
168 Heinrich (1999). The ablation was performed with spots of 40–50  $\mu\text{m}$  with a constant laser  
169 repetition rate of 10 Hz and a fluency of  $\sim 20$   $\text{J}/\text{cm}^2$  (Barca et al., 2011). Calibration was performed  
170 using the NIST 612-50 ppm glass reference material as external standard (Pearce et al., 1997).  
171 Internal standardization to correct instrumental instability and drift was achieved using CaO  
172 concentrations from EPMA-EDS analyses. Accuracy was evaluated on BCR 2G glass reference  
173 material and on an in-house pressed-powder cylinder of the standard Argillaceous Limestone  
174 SRM1d of NIST (Barca et al., 2011). The resulting element concentrations were compared with  
175 reference values from the literature (Gao et al., 2002). Accuracy, as the relative difference from

176 reference values, was always better than 12 %, and most elements plotted in the range of  $\pm 8$  %.  
177 Analyses were performed on 100  $\mu\text{m}$  thick cross-sections including both the black crust and the  
178 unaltered substrate samples in order to reveal the geochemical variability. TGA was carried out for  
179 the quantification of the carbonaceous fraction (TC total carbon= OC organic carbon + EC  
180 elemental carbon), Ox oxalate, CC carbonatic carbon and gypsum, present in the black crusts. It  
181 was performed by a Mettler Toledo TGA/DSC 3+, which allows simultaneous TG and DSC  
182 (Differential Scanning Calorimetry) analyses. The analyses were conducted in the range 30°- 800°  
183 C, increasing temperature with a rate of 20° C/minute. The carbonaceous components were  
184 estimated in temperature ranges defined by previously studied standards and using two different  
185 atmospheres, i.e. the inert and the oxidant one. The complete methodology is described also in  
186 previous works La Russa et al. (2017).

187

### 188 **3. Results and discussion**

#### 189 **3.1.POM Analysis**

190 Sample 2, coming from Salah El-Din citadel, is classified as biomicrite (Folk, 1959) and  
191 wackestone (Dunham, 1962). Moreover, quartz, iron oxides and macroforaminifera, i.e. nummulites  
192 (Khallaf, 2011) were also identified.

193 The crust overlapping the substrate is brownish in colour, has a roughly uniform thickness  
194 of about 175  $\mu\text{m}$ , it is composed by microcrystalline gypsum, brownish iron oxides and  
195 carbonaceous particles (Fig.1a).

196 The crust-substrate contact is rather clear with a marked separation between them.

197 The substrate in sample 3 is classified as biomicrite (Folk, 1959) or mudstone (Dunham, 1962). It  
198 includes allochems as quartz, rare iron oxides and fossils. The crust is located in small areas of the  
199 substrate and has a slightly variable thickness of about 20-30  $\mu\text{m}$ , containing iron oxides inside. It is  
200 well adhered to the substrate and appears with  
201 irregular and strongly discontinuous edges.

202 The substrates of samples 12 and 14 are classifiable as biomicrite (Folk, 1959) and mudstone  
203 (Dunham, 1962).

204 In particular, the substrate of sample 12 includes rare quartz and plagioclase crystals. The black  
205 crust overlying the substrate is rather compact with an overall thickness varying between 50 and  
206 200  $\mu\text{m}$ . It shows a not so clear stratification but at least two layers are recognizable. The crust is  
207 well adhered to the substrate, has irregular morphology, is made up of microcrystalline gypsum and  
208 incorporates numerous spherical and sub-spherical carbonaceous particles.

209 In sample 14, the crust has an average thickness of 400  $\mu\text{m}$  and shows an evident stratification  
210 (Fig.1b): an external dark brown layer with an average thickness of 50  $\mu\text{m}$  and a rather regular  
211 external profile; an innermost layer, light brown in colour, reaching in some places a thickness of  
212 300  $\mu\text{m}$  and deepening into the substrate for about 100  $\mu\text{m}$ . The contact crust/substrate is mainly  
213 sharp.

214 The crust is made up of microcrystalline gypsum and includes from sub-spherical to spherical  
215 carbonaceous particles, particularly numerous, especially in the inner layer (Fig.1b) and averagely  
216 30  $\mu\text{m}$  in size.

217 Sample 15 is classified as biomicrite (Folk, 1959) and mudstone (Dunham, 1962). The crust is thick  
218 from 400 to 1000  $\mu\text{m}$ , and not well adhered to the substrate. It consists of microcrystalline gypsum  
219 and is layered in three levels (Fig. 1c): the outermost one shows a dark brown colour and an average  
220 thickness of 200  $\mu\text{m}$ ; the intermediate and the inner layers show a gradually lighter grey-brown  
221 colour and vary in thickness from 200 to 500  $\mu\text{m}$ . Carbonaceous particles are present throughout the  
222 thickness of the crust, but are noticeably abundant in the inner layer. They show a spherical-  
223 subspherical shape and a variable size from 20 to 50  $\mu\text{m}$

224 The substrate of samples B and E is biomicrite (Folk, 1959) and wackestone (Dunham, 1962) with  
225 bioclasts of considerable size exceeding 1mm (Fig.1d). The crust overlies regularly the limestone to  
226 which is well adhered; however, the morphology and thickness are rather irregular, the last one  
227 varying from 50 to 400  $\mu\text{m}$ .

228 The crust in sample B is constituted by microcrystalline gypsum and contains rare carbonaceous  
229 particles and iron oxides. It is possible to identify a darker brown outer layer, with a regular and  
230 thin thickness of about 20  $\mu\text{m}$ , and a brownish inner layer that has a greater and irregular thickness,  
231 from 50 to 300  $\mu\text{m}$  in the points where it deepens into the substrate.

232 The crust in sample E is discontinuous, with a variable thickness from 50 to 500  $\mu\text{m}$ , consists of  
233 microcrystalline gypsum and, at least, two irregular levels are distinguished (Fig. 1d): the outer one  
234 is browner and contains numerous carbonaceous particles; the internal layer, where present, is  
235 lighter and reddish, about 100  $\mu\text{m}$  thick and the carbonaceous particles are less common. The  
236 substrate of sample H is classified as biomicrite (Folk, 1959) and mudstone (Dunham, 1962). The  
237 allochem fraction includes quartz and macroforaminifera fragments.

238 Overall, the crust is fractured, jagged with very irregular edges (Fig. 1e). It also appears divided  
239 into two layers: the outermost dark coloured with a thickness of about 500  $\mu\text{m}$ , the innermost light  
240 grey with a thickness of 200  $\mu\text{m}$ . Microcrystalline gypsum, iron oxides and numerous carbonaceous  
241 particles are visible in both.

242

### 243 **3.2 XRD Analysis**

244 The analysis (Table 1S available in Supplementary material) revealed the presence of gypsum,  
245 calcite and secondarily quartz as the main mineralogical species in almost all the crusts examined.  
246 Quartz and calcite come from the limestone substrate, while gypsum is the main constituent of the  
247 crusts (Barca et al., 2011; Belfiore et al., 2013; La Russa et al., 2013b; Ruffolo et al., 2015). Among  
248 the other mineralogical phases, plagioclase, K-feldspar, hematite and clay minerals were identified  
249 in subordinate amount.

250 The crusts include halite, the most common sodium chloride salt in the subsurface water of Egypt  
251 and in sea spray coming from the Mediterranean Sea (Aly et al., 2015) and consequently also in  
252 Egyptian limestones (Gauri and Holdren, 1981; Gauri et al., 1986; Helmi, 1990). The salt is linked

253 to the capillary rise of water from the subsoil and the consequent precipitation of the salt inside the  
254 stone (Charola, 2000; Fitzner et al., 2002; Gomez-Heras and Fort, 2007).

255

### 256 **3.3 EPMA-EDS Analysis**

257 EPMA-EDS morphological and microchemical analyses were carried out on the black crusts of the  
258 five sites.

259 In the samples 2 and 3 the crusts show an irregular morphology. Compositional analysis revealed  
260 CaO as major component, followed by SO<sub>3</sub>, SiO<sub>2</sub>, Al<sub>2</sub>O<sub>3</sub>, ClO e FeO, Na<sub>2</sub>O, MgO, K<sub>2</sub>O.

261 Black crusts of samples 12-14 are adherent to the substrate, especially sample 12 (Fig. 2S a); they  
262 appear rather compact. Gypsum microcrystals and carbonaceous sub-spherical particles were  
263 identified.

264 The crusts are constituted mainly by CaO and SO<sub>3</sub> thanks to gypsum-based composition, secondly  
265 by SiO<sub>2</sub>, and lastly ClO, Al<sub>2</sub>O<sub>3</sub>, Na<sub>2</sub>O, MgO, K<sub>2</sub>O, FeO. In sample 12, gypsum was detected also in  
266 substrate, where the crust is thicker and deepens in.

267 The black crust in sample 15 shows a homogeneous morphology (Fig. 2S b). It does not properly  
268 adhere to the underlying substrate, due to the presence of numerous fractures, that in some points  
269 cross the entire body of the crust.

270 The most abundant component is mostly CaO, followed by SiO<sub>2</sub>, SO<sub>3</sub>, ClO, and lastly Al<sub>2</sub>O<sub>3</sub>, FeO,  
271 K<sub>2</sub>O, MgO, Na<sub>2</sub>O, TiO<sub>2</sub> and P<sub>2</sub>O<sub>5</sub>.

272 The crusts taken from Qaitbay Mosque show slight different morphological features.

273 Sample E is rather compact, with a regular external profile and a sharp contact with the substrate  
274 (Fig. 2S c). The crust in sample B is more porous with a dendritic morphology. It is adherent to the  
275 substrate except in some points, where the two portions are separated by fractures. In both crusts,  
276 acicular crystal of gypsum and sub-spherical carbonaceous particles were recognized.

277 The chemical analysis suggested how CaO is the predominant component, followed by SiO<sub>2</sub>, SO<sub>3</sub>,  
278 secondly by, ClO, Al<sub>2</sub>O<sub>3</sub>, Na<sub>2</sub>O, K<sub>2</sub>O, FeO and lastly by MgO, P<sub>2</sub>O<sub>5</sub> and TiO<sub>2</sub>.

279 The sample H shows in general an irregular morphology, fractures, and jagged edges. However, it  
280 was individuated little portions more homogeneous, compact and adherent to substrate, that were  
281 analysed by EDS and then by LA-ICP-MS. Gypsum microcrystals and carbonaceous particles were  
282 identified in the crust. The chemical composition is characterized by a high amount of CaO, Al<sub>2</sub>O<sub>3</sub>,  
283 SiO<sub>2</sub> and SO<sub>3</sub>, followed by Na<sub>2</sub>O, P<sub>2</sub>O<sub>5</sub>, K<sub>2</sub>O, and TiO<sub>2</sub>.

284

285

### 286 **3.4 LA-ICP-MS Analysis**

287

288 Trace elements concentrations were determined by LA-ICP-MS on the black crusts and underlying  
289 substrates of all the examined samples. The results obtained for each spot analysis are listed in  
290 Table 2S, where average values and corresponding standard deviations are displayed.

291 Looking at the concentrations of the most significant trace elements (Table 2S), elements like lead  
292 (Pb), barium (Ba), vanadium (V), chromium (Cr), cobalt (Co), zinc (Zn) and arsenic (As) have  
293 relatively high concentrations, indicating an accumulation of atmospheric pollutants on the gypsum  
294 crusts, regardless of the sampling location. The documented high concentrations of lead suggest that  
295 this element is still present in the urban environment of Cairo city many years after the ban of  
296 leaded gasoline in Egypt (Fujiwara et al., 2011), as it has been also shown by previous studies in  
297 other cities around the world (Sanjurjo Sánchez et al., 2011; Török et al., 2011; Graue et al., 2013).

298 As well known, all these elements can be introduced in the urban environment by a wide range of  
299 different anthropogenic processes, mainly mining, smelting, industrial manufacturing, metal  
300 processing, etc. (Johnson et al., 2011) but also by domestic and residential activities (heating,  
301 vehicles, transport). However, some elements occur naturally in the same urban environment as a  
302 result for example of geologic processes (erosion of outcropping bedrocks). The proportion of  
303 natural and anthropogenic components may vary widely depending thus on the geology and the  
304 industrial history of the urban centre. Our geochemical approach was addressed to define the



305 relation between pollution sources and degradation state of stone materials; for this purpose,  
306 Enrichment Factor was calculated both for heavy metals, metalloids and Rare Earths Elements  
307 (hereafter REE). Enrichment factors calculation is a procedure commonly used in geochemical  
308 studies for the determination of the anthropogenic origin of chemical elements. For the purpose of  
309 our study, the chemical procedure was followed by normalizing the chemical composition of trace  
310 elements in black crusts with respect to those of calcareous substrates on which they grew (Table  
311 3S).

312 The normalization procedure performed here used Scandium (Sc) as 'conservative' element, as it  
313 was presumed to have no anthropogenic enrichment or a minor anthropogenic input (Loring, 1991;  
314 Gallego et al., 2013). This calculation is carried out by comparing the concentrations of the trace  
315 elements with those of the conservative element by following the formula  $EF =$   
316  $(M/N)_{\text{sample}}/(M/N)_{\text{substrate}}$ , which is the ratio between the concentrations of the metal (M) and those  
317 of the normalizer (N), both for the sample and for substrate samples (Reimann and Caritat, 2000).  
318 Figure 2 show EFs for all the examined samples grouped for sampling location criterion. As shown  
319 in the Figure 2, samples 2 and 3 are enriched in Zn, As, Pb, REE (L-REE, light and H-REE, heavy)  
320 and Sn, Ba, Pb and HREE, respectively. Similarly, samples 12 and 14 show enrichment in all the  
321 LREE and in most metals and metalloids elements. The same enrichment trend (Fig. 2) is  
322 highlighted by the remaining samples (B, E, 15 and H).

323 Samples B and E reveal enrichments in Co, Mo, Sn, Sb, Ba, Pb, and Sn, Ba, Pb, respectively with  
324 associated null or slight enrichment in REE. As regards sample 15, metals and metalloids are  
325 similarly enriched as in the previous samples, while the REE show values close to the background.  
326 Conversely, sample H shows only a slight enrichment in Sn, Sb and Ba, with no enrichment in  
327 REE.

328 Finally, some heavy metal and metalloids concentrations (V, Cr, Co, Ni, Zn, As, Cd and Pb, Mn  
329 and Cu) in the studied black crusts were compared to the corresponding concentrations in road dust  
330 samples (after Abdel-Latif and Saleh, 2012), collected across the Cairo city (Fig. 3).

331 It is worth to note that Zn, Mn and Cu are, together with Fe (not determined in this study), the  
332 metals present in the higher concentrations in PM (Atzei et al., 2014). Road dust includes deposits  
333 and accumulates on ground surfaces, along roadsides, which is contaminated by heavy metals. It  
334 usually does not remain deposited in place for long, but it is easily re-suspended back into the  
335 atmosphere, as it was already mentioned. For the purposes of this work, the concentrations of the  
336 above-mentioned metals in the <125  $\mu\text{m}$  fraction were considered for the comparison as these sizes  
337 are easily resuspended in atmosphere contributing with a significant amount of trace elements in  
338 residential, main traffic roads and industrial areas. Metals concentrations in the dust were higher in  
339 main traffic roads and industrial areas compared to those of residential areas. Figure 3 shows the  
340 box plot diagram, in which minimum, maximum and average values for the selected elements in  
341 black crusts samples are reported together with the values corresponding to the metal concentration  
342 in the dust collected in Cairo (Abdel-Latif and Saleh, 2012). As can be seen, most of the heavy  
343 metal average values in the black crusts fall within the ranges relevant to the dust of the Cairo city.  
344 Exceptions in this trend are the value of arsenic (As) and, at lesser extent, the value of cadmium  
345 (Cd). In fact, black crusts samples experienced values of these two elements greater than those of  
346 dust samples. Both these metals have been widely used in industrial sector, i.e. man-made  
347 emissions from metal smelters (iron, steel, copper, lead and zinc production), mining activities,  
348 combustion processes (coal and oil) and refuse incineration (stabilizers and pigments in plastics).  
349 Studied black crusts may have accumulated these elements over time being considered as good  
350 traps for atmospheric particles, useful for the identification of the particulate matter pollution  
351 emission sources in urban areas.

352

### 353 **3.5 Carbonaceous fraction**

354 Carbonaceous particles emitted by combustion processes are among the main constituents of  
355 aerosol particulate matter (PM) (Bove et al., 2016; Bozzetti et al., 2017) and one of the main factors  
356 responsible for the blackening of buildings.

357 The quantification of the carbonaceous species that form the non-carbonatic fraction, i.e. OC  
358 (organic carbon) and EC (elemental carbon) in damage layers, are required particularly in urban  
359 areas in order to investigate atmospheric deposition processes on building surfaces, to get  
360 information on the possible particulate matter sources and to suggest mitigation measurements to  
361 fulfil a better conservation of the stone surfaces (Fermo et al., 2015).

362 Black carbon (also known as elemental carbon, EC, because of its structure quite similar to that of  
363 graphite) is emitted by combustion processes, such as traffic and biomass burning (Piazzalunga et  
364 al., 2010, 2011; Belis et al., 2011), and is the main responsible for soiling on monuments surfaces  
365 (Ghedini et al., 2000; Tidblad et al., 2012). On the other hand, OC that includes hundreds of organic  
366 substances of different nature, is emitted by combustion processes as a primary pollutant but is also  
367 of secondary origin and can form starting from gaseous organic precursors (i.e. volatile organic  
368 compounds, VOC) (Fuzzi et al., 2006; Robinson et al., 2007; Bernardoni et al., 2011; Gentner et al.,  
369 2012; Vassura et al., 2014; Daellenbach et al., 2016). It is also known that the Mediterranean region  
370 is characterized by an intense photochemistry during summer which brings to high concentration in  
371 the aerosol PM of secondary organic substances (Bozzetti et al., 2017) and this phenomenon in  
372 Cairo is particularly favoured.

373 Table 2 shows the values obtained by thermogravimetric analysis and reported as percentages by  
374 weight (wt.%) of TC (Total Carbon), OC (Organic Carbon); EC (Elemental Carbon); OX (Oxalate),  
375 Gy (Gypsum); OC/EC and EC/TC ratios are reported as well;  $TC=OC+EC$ .

376 At first sight, by comparing the samples taken from the same monument it is possible to highlight  
377 slight differences between them.

378 It should be noted that the greatest variability in the various samples was found for gypsum  
379 (minimum value of 9.7%, maximum value 51.25). In particular, the highest concentrations were  
380 obtained for samples 12, 14 and B in accordance with what was observed by XRD analysis.

381 In general, all the crust samples show higher EC values (wt. %) than OC (Table 2). The EC values  
382 are higher than what was generally observed for the samples of atmospheric particulate matter in

383 Cairo (Favez et al., 2008; Kanakidou et al., 2011; Lowenthal et al., 2014; Cheng et al., 2016). It is  
384 also important to stress out that the carbonaceous substances dominate the PM<sub>2.5</sub> composition of  
385 megacities atmosphere, especially in Cairo (Cheng et al., 2016).

386 Furthermore, data in the literature show that PM in the city of Cairo has an average annual OC/EC  
387 ratio of 2.45 (Lowenthal et al., 2014). This ratio is rather linked to seasonal conditions, with values  
388 of 3.45 (autumn season), 2.64 (winter season) and 2.17 for the summer season (Abu-Allaban et al.,  
389 2007). The highest levels observed during autumn season have been related to episodes of biomass  
390 combustion on the Nile delta. In fact, during this period of the year the residual straw from rice  
391 cultivation is commonly burned after the harvests. Carbonaceous particles emitted by this  
392 combustion could therefore partially reach the city thanks to the influence of prevailing winds from  
393 the North (Favez et al., 2008).

394 According to Kanakidou et al. (2011) the polluting sources contributing to the OC fraction into the  
395 air in Cairo are mainly represented by industry, residential, energy production and incinerators,  
396 while

397 EC is mainly emitted from mobile sources (diesel traffic) and combustion processes (e.g. domestic  
398 heating or industrial activities) (Abu-Allaban et al., 2007; Favez et al., 2008).

399 The obtained OC and EC values of the crust samples were compared with other black crust samples  
400 from Cairo taken, in some cases, from the same monuments (Rovella et al., 2020), whose study was  
401 focused on the state of conservation of the building materials. These data were obtained with the  
402 same TGA methodology and their use was essential to better understand the interaction between the  
403 polluted environment of Cairo city and the black crusts.

404 Figure 4 shows that, in general, as the sampling height of the crusts decreases, the concentration of  
405 EC increases. This confirms that the main source of this pollutant could be vehicle traffic which is  
406 responsible for the emission of particles which mainly affects surfaces at lower heights in direct  
407 contact with the road. The OC value on all the analysed samples varies from a minimum of 0.36 to  
408 a maximum of 1.88, while that of EC varies from a minimum of 0.99 to a maximum of 5.95. From

409 the trends shown in the Figure 4, it is also observed that the OC values are more constant than the  
410 EC values.

411 The clustering based on the relationship between the concentrations of EC and OC and showed in  
412 Figure 5a, suggest similar trends for most of the samples nevertheless they come from different  
413 areas of Cairo. The only exception is represented by site a) (Fig. 5b) where high EC values are  
414 observed especially for the relative three samples (samples 8, 9 and 10 of figure 5a which were both  
415 taken at low heights).

416 In order to evaluate potential differences on the accumulation of OC and EC within the crusts  
417 analysed in the city of Cairo and other polluted cities, comparisons were made with crusts taken  
418 from Italian monuments (Fig. 6) such as: Trevi Fountain in Rome (La Russa et al., 2017); several  
419 private buildings in Venice (La Russa et al., 2018), Church of Santa Maria delle Grazie in Milan  
420 (Comite and Fermo et al., 2018) and the Monza Cathedral located in the homonymous city (Comite  
421 et al., 2020c).

422 The comparison (Fig. 6a) allowed highlighting the presence of two types of samples for which quite  
423 good correlations between OC and EC were observed. Characteristic OC/EC ratios have been  
424 identified for the two groups corresponding to the angular coefficients of the trend lines: the first  
425 group has an OC/EC ratio = 0.47, while the second shows an OC/EC ratio = 0.42. This allows  
426 hypothesizing that for the second group, in which all the Cairo samples fall, the primary sources  
427 prevail while for the samples belonging to the first group, and a mixed contribution of the sources  
428 (primary + secondary) can be suggested. The high EC contents in the Cairo samples can be  
429 explained by a combination of various polluting sources such as mobile emissions or combustion  
430 processes (e.g. domestic heating or industrial activities) (Abu-Allaban et al., 2007; Favez et al.,  
431 2008).

432 In fact, the city is characterized by high congestion due to, as mention before, a population density  
433 of 13107/km<sup>2</sup> and 2.4 million cars (El-Mansy et al., 2013; CAPMAS, 2017; Moustafa et al., 2018).  
434 Urban growth rates are higher than the development rate of public transport services with a

435 consequent increase in the use of private vehicles and taxis (Duquennois and Newman, 2009; El-  
436 Dorghamy et al., 2015) which release a lot of black carbon into the air thus dominating the other  
437 potential polluting sources (Mahmoud et al., 2008). Vehicle traffic in the past has also been  
438 characterized by the presence of vehicles with old generation technical characteristics that have  
439 increased the pollution of the city (El Mowafi and Atalla, 2005; Kanakidou et al., 2011). Even in  
440 the past, domestic heating or industrial sector introduced significant quantities of black carbon into  
441 the air (Abu-Allaban et al., 2007; Favez et al., 2008). For these reasons, the first actions for  
442 environmental protection were introduced in the early 1990s and after that, a slight air quality  
443 improvement emerged (Kanakidou et al., 2011).

444 A further confirmation of our statement arises, comparing the OC/EC ratio (Fig. 6b) with that  
445 performed on the carbonaceous aerosols (Schauer et al., 1999, 2002; Saarikoski et al., 2008).  
446 Generally, relatively low values equal to or less than 1 are attributable to primary emissions and  
447 combustion of fossil fuels (Perrino et al., 2008), while ratios greater than 1 usually indicate different  
448 polluting emissions. Observing (see Table 2) the ratios (minimum value of 0.23 and maximum  
449 0.75) obtained for these samples, the polluting sources that have likely affected the accumulation of  
450 the carbonaceous fraction in the black crusts of Cairo are primary sources including vehicular road  
451 traffic.

452 In fact, it has been highlighted that for urban sites in Europe (Pio et al., 2011), where vehicular  
453 emissions are the dominant source of pollution, the values obtained from the OC/EC ratios fall in  
454 the range 0.3-0.7, suggesting a low contribution of secondary OC.

455 Finally, the correlation between the gypsum content, the carbonaceous fraction and the  
456 concentrations of heavy metals can provide further information on the sources of pollutants. Figure  
457 3S shows the correlation matrix between all the experimental variables quantified on the examined  
458 samples in the present paper. The observation of the matrix shows how gypsum is positively related  
459 to different heavy metals, namely Cu, Pb, Sb and Zn, and to, a lesser extent, the remaining metals  
460 and metalloids. This could indicate that probably some elements are closely related to the

461 sulphation processes. In fact, heavy metals have long been considered capable of catalysing the  
462 sulphation processes (Rodriguez-Navarro and Sebastian, 1996; Cultrone et al., 2004; Simaõ et al.,  
463 2006; Wahba and Zaghoul, 2007). A good correlation has been observed between Gy and Cu  
464 (0.92). According to Boke et al. (1999), the  $\text{Cu}^{+2}$  ion increases the absorption of  $\text{SO}_2$  in the aqueous  
465 film present on a carbonate surface. This ion has also been shown to dissipate any gradient of  
466 electrical potential allowing hydrogen ions to spread much faster on surfaces (Chang et al., 1981).  
467 As a result, an increase in  $\text{SO}_2$  uptake is observed which accelerates the sulphation process.  
468 Furthermore, Cu has been shown to be released from the exchangeable carbonate phase making this  
469 metal potentially available to catalyse surface reactions (McAlister et al., 2008).

470 The correlation matrix also allows highlighting the correlation existing between metals. For  
471 example, there is a very good correlation between Ni and V indicating the contribution of heavy oil  
472 combustions (Bove et al., 2016).

473 On the contrary, the carbonaceous fraction EC is negatively correlated with gypsum and also with  
474 various heavy metals. In fact, the surface of EC particles contains numerous adsorption sites that are  
475 capable of enhancing catalytic processes because of their high surface reactivity. As result of its  
476 catalytic properties, EC may affect some important chemical reactions involving atmospheric  
477 sulphur dioxide ( $\text{SO}_2$ ), nitrogen oxides ( $\text{NO}_x$ ), ozone ( $\text{O}_3$ ) and other gaseous compounds (Gundel et  
478 al., 1989) other than could have a catalytic effect on the oxidation of sulphite to sulphate (Böke et  
479 al., 1999).

480 As observed in the figure 3, where the greatest polluting contribution seem to be linked to vehicle  
481 traffic along the major road arteries, it is clear that the pollution produced by vehicles could also be  
482 the main source of enrichment of black crusts.

483

484

485

486

#### 487 **4. Conclusion**

488 The results achieved in this work highlighted the strong correlation between the atmosphere  
489 composition and the degradation processes affecting stone materials used in the built cultural  
490 heritage of Cairo city. The multi-analytical approach demonstrated how black crusts can be  
491 considered such as an efficient “natural sample holder” of atmospheric pollutants, capable to  
492 provide information about atmospheric composition especially in terms of heavy metals. Precisely,  
493 the study revealed that the black crusts analysed are constituted mainly by heavy minerals  
494 ascribable to the road dust of Cairo city, with the exception of As and Cd, being widely used in the  
495 industrial sector.

496 The data on the carbonaceous fraction suggested that the formation of black crusts sampled is  
497 influenced by a preeminent action of the primary sources. At the same time, the high EC contents  
498 confirmed the contribution of various polluting sources, such as mobile emissions or combustion  
499 processes (e.g. domestic heating or industrial activities) in the formation of the black crusts.  
500 Additionally, EC data affirm the clear predominance of pollution produced by vehicles, becoming  
501 the main source of enrichment of the black crusts.

502 In particular, the sulphation processes in the Cairo city is improved by heavy metals, i.e. Cu, Pb, Sb  
503 and Zn that play a catalysing role.

504 This research demonstrated how the contribution of atmospheric pollution is crucial in the evolution  
505 of the degradation phenomena, affecting the built cultural heritage in Historic Cairo. Consequently,  
506 the reduction of emissions into the atmosphere, adopting for example more eco-sustainable policies,  
507 becomes extremely necessary not only for the conservation of cultural heritage but more in general,  
508 for the safeguard of the environment and human health.

509

#### 510 **Acknowledgements**



511 The present research is a part of an Executive program for scientific cooperation between the Italian  
512 Republic and the Arab Republic of Egypt, entitled “Characterization of black crusts formed on  
513 historical buildings under different levels of ambient air pollution in Cairo and Venice”.

514 Moreover, it is also part of an international cooperation program funded by CSIC, I-COOP  
515 (“Implementation of a reference laboratory for the diagnosis, conservation and restoration of stone-  
516 cultural heritage in Egypt”, January 2019 December 2020, Ref. COOPB20379).

517 Finally, the research was partially funded by the project TOP Heritage (P2018/NMT-4372) of the  
518 Community of Madrid. The authors wish to acknowledge professional support of the  
519 Interdisciplinary Thematic Platform from CSIC Open Heritage: Research and Society (PTI-PAS).

520

521

522

523

524

525

526

## 527 **References**

528           Abbass, R.A., Kumar, P.T., El-Gendy, A., 2020. Car users exposure to particulate matter and  
529 gaseous air pollutants in megacity Cairo. *Sustain. Cities Soc.* 56 (102090), 1-13.  
530 <https://doi.org/10.1016/j.scs.2020.102090>.

531           Abdel-Latif, N.M., Saleh, I.A., 2012. Heavy Metals Contamination in Roadside Dust along Major  
532 Roads and Correlation with Urbanization Activities in Cairo, Egypt. *J. Am. Sci.* 8(6), 379-389. ISSN: 1545-  
533 1003.

534           Abdelmegeed, M., Hassan, S., 2019. Diagnostic investigation of decaying limestone in historical  
535 buildings at the Mamluks Cemetery - City of the Dead, Egypt. *EJARS* 9(2), 183-196.

536 DOI: 10.21608/ejars.2019.66989.

537 Abu-Allaban, M., Lowenthal, D.H., Gertler, A.W., Labib, M., 2007. Sources of PM10 and PM2.5 in  
538 Cairo's ambient air. *Environ. Monit. Assess* 133, 417–425. <https://doi.org/10.1007/s10661-006-9596-8>.

539 Abu-Allaban, M., Lowenthal, D.H., Gertler, A.W., Labib, M., 2009. Sources of volatile organic  
540 compounds in Cairo's ambient air. *Environ. Monit. Assess.* 157, 179–189.  
541 DOI 10.1007/s10661-008-0526-9.

542 Ahmed, H., Torok, A., Locsei, J., 2006. Performance of some commercial consolidating agents on  
543 porous limestones from Egypt “Tura and Mokattam Quarry”. In: *Heritage, Weathering and Conservation: Proceedings of the International Heritage, Weathering And Conservation Conference (HWC-2006)*, 21-24  
544 June 2006 Madrid, Spain, pp. 735-740.

546 Alkhdhairi, S.A., Abdel-Hameed, U.K., Morsy, A.A., Tantawy, M.E., 2018. Air Pollution and its  
547 Impact on the Elements of Soil and Plants in Helwan Area. *Int. J. Adv. Res. Biol. Sci.* 5(6), 38-59  
548 <http://dx.doi.org/10.22192/ijarbs.2018.05.06.004>.

549 Aly, N., Hamed, A., Gomez-Heras, M., Alvarez de Buergo, M., 2015. The influence of temperature  
550 in a capillary imbibition salt weathering simulation test on Mokattam limestone. *Mater. Construc.* 65 (317).  
551 <https://doi.org/10.3989/mc.2015.00514>.

552 Aly, N., Hamed, A., Abd El-Al, A., 2020. The impact of hydric swelling on the mechanical behavior  
553 of Egyptian Helwan Limestone. *Period. Polytech. Civ.* 64(2), 589-596. <https://doi.org/10.3311/PPci.15360>.

554 Atzei, D., Fantauzzi, M., Rossi, A., Fermo, P., Piazzalunga, A., Valli, G., Vecchi, R., 2014. Surface  
555 chemical characterization of PM10 samples by XPS. *Appl. Surf. Sci.* 307, 120-128.  
556 <https://doi.org/10.1016/j.apsusc.2014.03.178>.

557 Barca, D., Belfiore, C.M., Crisci, G.M., La Russa, M.F., Pezzino, A., Ruffolo, S.A., 2011. A new  
558 methodological approach for the chemical characterization of black crusts on building stones: a case study  
559 from the Catania city centre (Sicily, Italy). *J. Anal. At. Spectrom.* 26, 1000–1011.  
560 <https://doi.org/10.1039/C0JA00226G>.

561 Belfiore, C.M., Barca, D., Bonazza, A., Comite, V., La Russa, M.F., Pezzino, A., Ruffolo, S.A.,  
562 Sabbioni, C., 2013. Application of spectrometric analysis to the identification of pollution sources causing  
563 cultural heritage damage. *Environ. Sci. Pollut. Res.* 20, 8848–59. <https://doi.org/10.1007/s11356-013-1810->  
564 y.

565 Belis, C.A., Cancelinha, J., Duane, M., Forcina, V., Pedroni, V., Passarella, R., Tanet, G., Douglas,  
566 K., Piazzalunga, A., Bolzacchini, E., Sangiorgi, G., Perrone, M.G., Ferrero, L., Fermo P., Larsen, B.R., 2011.  
567 Sources for PM air pollution in the Po Plain, Italy: I. Critical comparison of methods for estimating biomass  
568 burning contributions to benzo(a) pyrene. *Atmos. Environ.* 45(39), 7266–7275.  
569 <https://doi.org/10.1016/j.atmosenv.2011.08.061>.

570 Bernardoni, V., Vecchi, R., Valli, G., Piazzalunga, A., Fermo P., 2011. PM10 source apportionment  
571 in Milan (Italy) using time-resolved data. *Sci. Tot. Environ.* 409, 4788–4795.  
572 <https://doi.org/10.1016/j.scitotenv.2011.07.048>.

573 Böke, H., Göktürk, E.H., Caner-Saltık, E.N., Demircia, Ş., 1999. Demirci Effect of airborne particle  
574 on SO –calcite reaction. *Appl. Surf. Sci.* 140 (1-2), 70–82. [https://doi.org/10.1016/S0169-4332\(98\)00468-1](https://doi.org/10.1016/S0169-4332(98)00468-1).

575 Borai, E.H., Soliman, A.A., 2001. Monitoring and statistical evaluation of heavy metals in airborne  
576 particulates in Cairo, Egypt. *J. Chromatogr. A.* 920(1-2), 261-269. [https://doi.org/10.1016/S0021-](https://doi.org/10.1016/S0021-9673(01)00857-3)  
577 [9673\(01\)00857-3](https://doi.org/10.1016/S0021-9673(01)00857-3).

578 Bove, M.C., Brotto, P., Calzolari, G., Cassola, F., Cavalli, F., Fermo, P., Hjorth, J., Massabò, D.,  
579 Nava, S., Piazzalunga, A., Schembari, C., Prati P., 2016. PM10 source apportionment applying PMF and  
580 chemical tracer analysis to ship-borne measurements in the Western Mediterranean. *Atmos. Environ.* 125,  
581 140-151. <https://doi.org/10.1016/j.atmosenv.2015.11.009>.

582 Bozzetti, C., El Haddad, I., Salameh, D., Daellenbach, K.R., Fermo, P., Gonzalez, R., Minguillón,  
583 M.C., Iinuma, Y., Poulain, L., Elser, M., Müller, E., Slowik, J.G., Jaffrezo, J.L., Baltensperger, U.,  
584 Marchand, N., Prévôt, A.S.H., 2017. Organic aerosol source apportionment by offline-AMS over a full year  
585 in Marseille. *Atmos. Chem. Phys.* 17(13), 8247-8268. <https://doi.org/10.5194/acp-17-8247-2017>.

586 CAPMAS, 2017. Inventory of licensed vehicles for 2016. Cairo, Egypt: Central Agency for Public  
587 Mobilization and Statistics No. 71-21315-2016. <https://www.capmas.gov.eg>, last accessed: 18 June 2020.

588 Charola, A.E., 2000. Salts in the Deterioration of Porous Materials: An Overview. *J. Am. Inst.*  
589 *Conservat.* 39(3), 327-343. <https://doi.org/10.1179/019713600806113176>.

590 Chang, C.S., Rochelle, G.T., 1981. SO<sub>2</sub> absorption into aqueous solutions. *AIChE J.* 27(2), 292–298.

591 Cheng, Z., Luo, L., Wang, S., Wang, Y., Sharma, S., Shimadera, H., Wang, X., Bressi, M., De  
592 Miranda, R.M., Jiang, J., Zhou, W., Fajardo, O., Yan, N., Hao, J., 2016. Status and characteristics of ambient

593 PM2.5 pollution in global megacities. *Environ. Int.* 89–90, 212–221.  
594 <https://doi.org/10.1016/j.envint.2016.02.003>.

595 Comite, V., Barca, D., Belfiore, C.M., Bonazza, A., Crisci, G.M., La Russa, M.F., Pezzino, A.,  
596 Sabbioni, C., 2012. Potentialities of spectrometric analysis for the evaluation of pollution impact in  
597 deteriorating stone heritage materials. In: *Rendiconti online della Società Geologica Italiana*, 86 Congresso  
598 Nazionale della Società Geologica Italiana, Arcavacata di Rende, 18–20 September 2012, Roma, vol. 21, pp.  
599 652–653.

600 Comite, V., Fermo, P., 2018. The effects of air pollution on cultural heritage: the case study of Santa  
601 Maria delle Grazie al Naviglio Grande (Milan). *E.P.J. Plus.* 133 (12), 556-566.  
602 <https://doi.org/10.1140/epjp/i2018-12365-6>.

603 Comite, V., Pozo-Antonio, J.S., Cardell, C., Rivas, T., Randazzo, L., La Russa, M.F., Fermo, P.,  
604 2019. Metals distributions within black crusts sampled on the facade of an historical monument: The case  
605 study of the Cathedral of Monza (Milan, Italy). In: *IMEKO TC4 International Conference on Metrology for  
606 Archaeology and Cultural Heritage (MetroArchaeo)*, 04 - 06 December 2019, Florence, pp.73-78.

607 Comite, V., Ricca, M., Ruffolo, S.A., Graziano, S.F., Rovella, N., Rispoli, C., Gallo, C., Randazzo,  
608 L., Barca, D., Cappelletti, P., La Russa, M.F., 2020a. Multidisciplinary approach to evaluate the geochemical  
609 degradation of building stone related to pollution sources in the Historical Centre of Naples (Italy). *Int. J.*  
610 *Conserv. Sci.* 11(1), 291-304. <https://doi.org/10.3390/app10124241>.

611 Comite, V., Pozo-Antonio, J.S., Cardell, C., Rivas, T., Randazzo, L., La Russa, M.F., Fermo, P.,  
612 2020b. Environmental impact assessment on the Monza cathedral (Italy): a multi-analytical approach. *Int. J.*  
613 *Conserv. Sci.* 11(1), 291-304.

614 Comite, V., Pozo-Antonio, J.S., Cardell, C., Randazzo, L., La Russa, M.F., Fermo, P., 2020c. A  
615 multi-analytical approach for the characterization of black crusts on the facade of an historical cathedral.  
616 *Microchem. J.* 158, 105121. <https://doi.org/10.1016/j.microc.2020.105121>.

617 Creighton, P.J., Liroy, P.J., Haynie, F.H., Lemmons, T.J., Miller, J.L., Gerhart, J., 1990. Soiling by  
618 Atmospheric Aerosols in an Urban Industrial Area. *J. Air Waste Manag. Assoc.* 40(9), 1285-1289.  
619 <https://doi.org/10.1080/10473289.1990.10466783>.

620 Cultrone, G., Rodriguez-Navarro, C., Sebastian, E., 2004. Limestone and brick decay in simulated  
621 polluted atmosphere: the role of particulate matter, in: Siaz-Jimenez, C. (Eds.), *Air Pollution and Cultural*  
622 *Heritage*. Balkema A.A. Publishers, Leiden, London, New York, Philadelphia, Singapore, pp. 141–145.

623 Daellenbach, K.R., Bozzetti, C., Křepelová, A., Canonaco, F., Wolf, R., Zotter, P., Fermo, P.,  
624 Crippa, M., Slowik, J.G., Sosedova, Y., Zhang, Y., Huang, R.J., Poulain, L., Szidat, S., Baltensperger, U., El  
625 Haddad, I., Prévôt, A.S.H., 2016. Characterization and source apportionment of organic aerosol using offline  
626 aerosol mass spectrometry. *Atmos. Meas. Tech.* 9(1), 23–39. <https://doi.org/10.5194/amt-9-23-2016>.

627 Davidson, C.I., Tang, F., Finger, S., Etyemezian, V., Sherwood, S.I., 2000. Soiling patterns on a tall  
628 limestone building: changes over 60 years. *Environ. Sci. Technol.* 34(4), 560–565.  
629 <https://doi.org/10.1021/es990520y>.

630 Dunham, R.J., (1962). Classification of carbonate rocks according to depositional textures. *Amer.*  
631 *Assoc. Petrol. Geol. Mem.* 1, 108-121.

632

633 Duquennois, A.N., Newman, P., 2009. Linking the green and brown agendas: A case study on Cairo,  
634 Egypt. UN habitat, global report on human settlements. <http://www.unhabitat.org/grhs/2009>, last accessed:  
635 24 June 2020.

636 El-Dorghamy, A., Allam, H., Al-Abyad, A., Gasnier, M., 2015. Fuel economy and CO2 emissions of  
637 light-duty vehicles in Egypt. Centre for Environment and Development in the Arab Region and Europe  
638 (CEDARE). <http://web.cedare.org/>, last accessed: 20 June 2020.

639 El Mowafí, S.A., Atalla, A.G., 2005. Strategies for controlling mobile emissions in Cairo. *Manag.*  
640 *Environ. Qual.* 16(5), 548-559. <https://doi.org/10.1108/14777830510614385>.

641 El-Nahas, F., Moustafa, A., Abdel-Tawab, S., 1990. Geotechnical characteristics of limestone  
642 formations of Gebel Mokattam area. *Proceedings of First Alexandria Conference on Structural and*  
643 *Geotechnical Engineering*, Alexandria University, Egypt, vol. 1, pp. 9-19.

644 El-Tawab, N.A., Mahran, A., Badr, I., 2012. Restoration and preservation of the wooden ceiling of  
645 Al-Ashraf Qaytbay madressa, Cairo Egypt. *EJARS* 2(1), 11-28. doi: 10.21608/ejars.2012.7456

646 El-Mansy, A., Heikal, A., Abo Taleb A., 2013. Integration of GPS and GIS to study traffic  
647 congestion on Cairo Road network to minimize the harmful environmental effects. Case study (autostrad

648 Road). Partial fulfilment of the requirement for the master degree. Cairo Egypt: Ain Shams University,  
649 Lambert Academic Publishing, Cairo.

650 Favez, O., Cachiera, H., Sciare, J., Alfaro, S.C., El-Araby, T.M., Harhash, M.A., Abdelwahab,  
651 M.M., 2008. Seasonality of major aerosol species and their transformations in Cairo megacity. *Atmos.*  
652 *Environ.* 42, 1503–1516. <https://doi.org/10.1016/j.atmosenv.2007.10.081>.

653 Fermo, P., Turrion, R.G., Rosa, M., Omegna, A., 2015. A new approach to assess the chemical  
654 composition of powder deposits damaging the stone surfaces of historical monuments. *Environ. Sci. Pollut.*  
655 *Res.* 22, 6262-6270. <https://doi.org/10.1007/s11356-014-3855-y>.

656 Fermo, P., Comite, V., Ciantelli, C., Sardella, A., Bonazza, A., 2020. A multi-analytical approach to  
657 study the chemical composition of total suspended particulate matter (TSP) to assess the impact on urban  
658 monumental heritage in Florence. *Sci. Total. Environ.* 740-140055.

659 Fitzner, B., Heinrichs, K., La Bouchardiere, D., 2002. Weathering damage on Pharaonic sandstone  
660 monuments in Luxor-Egypt. *Build Environ* 38, 1089-1103. DOI: 10.1016/S0360-1323(03)00086-6.

661 Folk, R.L., 1959. Practical petrographic classification of limestones. *Bull. Amer. Assoc. Petrol.*  
662 *Geol.* 43, 1-38. <https://doi.org/10.1306/0BDA5C36-16BD-11D7-8645000102C1865D>.

663 Fujiwara, F., Rebagliati, R.J., Dawidowski, L., Gómez, D., Polla, G., Pereyra, V., Smichowski, P.,  
664 2011. Spatial and chemical patterns of size fractionated road dust collected in a megacity. *Atmos. Environ.*  
665 45, 1497-1505. <https://doi.org/10.1016/j.atmosenv.2010.12.053>.

666 Fuzzi, S., Andreae, M.O., Hueber, B.J., Kulmala, M., Bon, T.C., Boy, M., Doherty, S.J., Guenther,  
667 A., Kanakidou, M., Kawamura, K., Kerminen, V.M., Lohmann, U., Russell, L.M., Poschl, U., 2006. Critical  
668 assessment of the current state of scientific knowledge, terminology, and research needs concerning the role  
669 of organic aerosols in the atmosphere, climate, and global change. *Atmos. Chem. Phys.* 6, 2017–2038.  
670 <https://doi.org/10.5194/acp-6-2017-2006>.

671 Gallego, J.R., Ortiz, J.E., Sierra, C., Torres, T., Llamas, J.F., 2013. Multivariate study of trace  
672 element distribution in the geological record of Roñanzas Peat Bog (Asturias, N. Spain).  
673 Palaeoenvironmental evolution and human activities over the last 8000 cal yr BP. *Sci. Total Environ.* 454,  
674 16-29. <https://doi.org/10.1016/j.scitotenv.2013.02.083>.

675 Gao, S., Liu, X., Yuan, H., Hattendorf, B., Gunther, D., Chen, L., Hu, S., 2002. Determination of  
676 forty two major and trace elements in USGS and NIST SRM glasses by laser ablation-inductively coupled  
677 plasma mass spectrometry. *Geostandard Newslett.* 26, 181–196. [https://doi.org/10.1111/j.1751-](https://doi.org/10.1111/j.1751-908X.2002.tb00886.x)  
678 [908X.2002.tb00886.x](https://doi.org/10.1111/j.1751-908X.2002.tb00886.x).

679 Gauri, K.L., Holdren, G.C., 1981. Deterioration of the stone of the Great Sphinx. *ARCE Newsletter*,  
680 114, 35-47.

681 Gauri, K.L., Holdren, G.C., Vaughan, W.C., 1986. Cleaning Efflorescences from Masonry, in:  
682 Clifton, J.R. (ed.), *Cleaning Stone and Masonry*. American Society for Testing and Materials, Philadelphia,  
683 pp. 3-13.

684 Gentner, D.R., Isaacman, G., Worton, D.R., Chan, A.W.H., Dallmann, T.R., Davisa, L., Liud, S.,  
685 Day, D.A., Russell, L.M., Wilson, K.R., Weber, R., Guha, A., Harley, R.A., Goldstein, A.H., 2012.  
686 Elucidating secondary organic aerosol from diesel and gasoline vehicles through detailed characterization of  
687 organic carbon emissions. *Proc. Natl. Acad. Sci. U.S.A.* 109, 18318–18323.  
688 <https://doi.org/10.1073/pnas.1212272109>.

689 Ghedini, N., Gobbi, G., Sabbioni, C., Zappia, G., 2000. Determination of elemental and organic  
690 carbon on damaged stone monuments. *Atmos. Environ.* 34(25), 4383-4391. [https://doi.org/10.1016/S1352-](https://doi.org/10.1016/S1352-2310(00)00250-8)  
691 [2310\(00\)00250-8](https://doi.org/10.1016/S1352-2310(00)00250-8).

692 Gomez-Heras, M., Fort, R., 2007. Patterns of halite (NaCl) crystallisation in building stone  
693 conditioned by laboratory heating regimes. *Environ. Geol.* 52, 259–267. [https://doi.org/10.1007/s00254-006-](https://doi.org/10.1007/s00254-006-0538-0)  
694 [0538-0](https://doi.org/10.1007/s00254-006-0538-0).

695 Graue, B., Siegesmund, S., Oyhantcabal, P., Naumann, R., Licha, T., Simon, K., 2013. The effect of  
696 air pollution on stone decay: the decay of the Drachenfels trachyte in industrial, urban, and rural  
697 environments—a case study of the Cologne, Altenberg and Xanten cathedrals. *Environ. Earth Sci.* 69, 1095–  
698 1124. <https://doi.org/10.1007/s12665-012-2161-6>.

699 Gundel, L.A., Guyot-Sionnest, N.S., Novakov, T., 1989. A study of the interaction of NO<sub>2</sub> with  
700 carbon particles. *Aerosol Sci. Tech.* 10(2), 343-351. <https://doi.org/10.1080/02786828908959271>.

701 Gunther, D., Heinrich, C.A., 1999. Enhanced sensitivity in laser ablation-ICP mass spectrometry  
702 using helium-argon mixtures as aerosol carrier. *J. Anal. At. Spectrom.* 14, 1363-1368.  
703 <https://doi.org/10.1039/A901648A>

704 Gurjar, B.R., Nagpure, A.S., Singh, T.P., Hanson, H., 2010. Air quality in megacities, in: Cleveland,  
705 C.J. (Eds.), *Encyclopedia of Earth. Environmental Information Coalition, National Council for Science and*  
706 *the Environment.* Washington D.C. [http://www.eoearth.org/article/Air\\_quality\\_in\\_mega\\_cities](http://www.eoearth.org/article/Air_quality_in_mega_cities).

707 Helmi, F.M., 1990. Study of salt problem in the sphinx, Giza, Egypt. In: 9th Triennial meeting,  
708 ICOM Committee for Conservation, 26-31 August 1990, vol.1, Dresden, Germany. Grimstad, K. (Ed.),  
709 ICOM Committee for Conservation, Los Angeles, pp. 326-329.

710 Johnson, C.C., Demetriades, A., Locutura, J., Ottesen, R.T., 2011. *Mapping the Chemical*  
711 *Environment of Urban Areas.* Wiley, New York City, United States, ISBN: 978-0-470-74724-7, 640 Pages.

712 Kanakidou, M., Mihalopoulos, N., Kindap, T., Im, U., Vrekoussis, M., Gerasopoulos, E.,  
713 Dermizaki, E., Unal, A., Koçak, M., Markakis, K., Melas, D., Kouvarakis, G., Youssef, A.F., Richter, A.,  
714 Hatzianastassiou, N., Hilboll, A., Ebojie, F., Wittrock, F., von Savigny, C., Burrows, J.P., Ladstaetter-  
715 Weissenmayer, A., Moubasher, H., 2011. Review Megacities as hot spots of air pollution in the East  
716 Mediterranean. *Atmos. Environ.* 45(6), 1223-1235. <https://doi.org/10.1016/j.atmosenv.2010.11.048>.

717 Khairy, M.A., Barakat, A.O., Mostafa, A.R., Wade, T.L., 2011. Multielement determination by  
718 flame atomic absorption of road dust samples in Delta Region, Egypt. *Microchem. J.* 97(2), 234-242.  
719 <https://doi.org/10.1016/j.microc.2010.09.012>.

720 Khallaf, M.K., 2011. Effect of Air Pollution on Archaeological Buildings in Cairo, in: Chmielewski,  
721 A. (Eds.), *Monitoring, Control and Effects of Air Pollution.* IntechOpen, London, pp. 179-200.  
722 <https://doi.org/10.5772/16748>.

723 Köppen, W., Geiger R., 1930. *Handbuch der Klimatologie,* Gebrueder Borntraeger (Eds.), Berlin.

724 Kukela, A., Segliņš, V., 2011. Simplified Method of Assessment of Weathering on Historical Stone  
725 Monuments: An Example of El-Merdani Mosque, Cairo, Egypt. *J. Earth Sci. Eng.* 1, 82-90.

726 La Russa, M.F., Ruffolo, S.A., Belfiore, C.M., Aloise, P., Randazzo, L., Rovella, N., Pezzino, A.,  
727 Montana, G., 2013a. Study of the effects of salt crystallization on degradation of limestone rocks.  
728 *Period. Mineral.* 82(1), 113-127. <http://dx.doi.org/10.2451/2013PM0007>.



729 La Russa, M.F., Belfiore, C.M., Comite, V., Barca, D., Bonazza, A., Ruffolo, S.A., Crisci, G.M.,  
730 Pezzino, A., 2013b. Geochemical study of black crusts as a diagnostic tool in cultural heritage. *Appl. Phys.*  
731 *A Mater.* 113, 1151–62. <https://doi.org/10.1007/s00339-013-7912-z>.

732 La Russa, M.F., Fermo, P., Comite, V., Belfiore, C.M., Barca, D., Cerioni, A., De Santis, M.,  
733 Barbagallo, L.F., Ricca, M., Ruffolo, S. A., 2017. The Oceanus statue of the Fontana di Trevi (Rome): The  
734 analysis of black crust as a tool to investigate the urban air pollution and its impact on the stone degradation.  
735 *Sci. Total. Environ.*, 593-594, 297-309. <https://doi.org/10.1016/j.scitotenv.2017.03.185>.

736 La Russa, M.F., Comite, V., Aly, N., Barca, D., Fermo, P., Rovella, N., Antonelli, F., Tesser, E.,  
737 Aquino, M., Ruffolo, S.A., 2018. Black crusts on Venetian built heritage, investigation on the impact of  
738 pollution sources on their composition. *Eur. Phys. J. Plus* 133, 370. [https://doi.org/10.1140/epjp/i2018-](https://doi.org/10.1140/epjp/i2018-12230-8)  
739 12230-8.

740 Loring, D.H., 1991. Normalization of heavy-metal data from estuarine and coastal sediments.  
741 *ICES J. Mar. Sci.* 48(1), 101-115. <https://doi.org/10.1093/icesjms/48.1.101>.

742 Lowenthal, D.H., Gertler, A.W., Labib, M.W., 2014. Particulate matter source apportionment in  
743 Cairo: recent measurements and comparison with previous studies. *Int. J. Environ. Sci. Technol.* 11 (3), 657–  
744 670. <https://doi.org/10.1007/s13762-013-0272-6>.

745 Mahmoud, K.F., Alfaro, S.C., Favez, O., Abdel Wahab, M.M., Sciare, J., 2018. Origin of black  
746 carbon concentration peaks in Cairo (Egypt). *Atmos. Res.* 89 (1-2), 161–169.  
747 <https://doi.org/10.1016/j.atmosres.2008.01.004>.

748 McAlister, J.J., Smitha, B.J., Török, A., 2008. Transition metals and water-soluble ions in deposits  
749 on a building and their potential catalysis of stone decay. *Atmos. Environ.* 42 (33), 7657–68.  
750 <https://doi.org/10.1016/j.atmosenv.2008.05.067>.

751 Mostafa, A.N., Zakey, A.S., Monem, A.S., Wahab M.M.A., 2018. Analysis of the surface air quality  
752 measurements in the Greater Cairo (Egypt) metropolitan. *GJAR*, 5(6), 207–214.

753 Orphy, M., Hamid, A., 2004. Problems Islamic monuments in Cairo face. In: 13th International  
754 Brick and Block Masonry Conference Amsterdam, July 4-7, 2004. Martens, D.R.W., Vermeltfoort, A.T.  
755 (Eds). Eindhoven: Technische Universiteit Eindhoven.

756 Park, H.D., Shin, G.H., 2009. Geotechnical and geological properties of Mokattam limestones:  
757 Implications for conservation strategies for ancient Egyptian stone monuments. *Eng. Geol.* 104(3–4),190-  
758 199. <https://doi.org/10.1016/j.enggeo.2008.10.009>

759 Pearce, N.J.G., Perkins, W.T., Westgate, J.A., Gorton, M.P., Jackson, S.E., Neal, C.R., Chenery,  
760 S.P., 1997. A compilation of new and published major and trace element data for NIST SRM 610 and NIST  
761 SRM 612 glass reference materials. *Geostandard Newslett.* 21, 115–144. <https://doi.org/10.1111/j.1751-908X.1997.tb00538.x>.

763 Perrino, C., Canepari, S., Catrambone, M., Dalla Torre, S., Rantica, E., Sargolini, T., 2009. Influence  
764 of natural events on the concentration and composition of atmospheric particulate matter. *Atmos. Environ.*  
765 43, 4766–4779. <https://doi.org/10.1016/j.atmosenv.2008.06.035>.

766 Piazzalunga, A., Fermo, P., Bernardoni, V., Vecchi, R., Valli, G., De Gregorio, M., 2010. A  
767 simplified method for levoglucosan quantification in wintertime atmospheric particulate matter by high  
768 performance anion-exchange chromatography coupled with pulsed amperometric detection. *Int. J. Environ.*  
769 *Anal. Chem.* 90, 934–947. <http://dx.doi.org/10.1080/03067310903023619>.

770 Piazzalunga, A., Belis C., Bernardoni, V., Cazzuli, O., Fermo, P., Valli, G., Vecchi, R., 2011.  
771 Estimates of wood burning contribution to PM by the macro-tracer method using tailored emission factors.  
772 *Atmos. Environ.* 45, 6642–6649. <https://doi.org/10.1016/j.atmosenv.2011.09.008>.

773 Pio, C.A., Legrand, M., Oliveira, T., Afonso, J., Santos, C., Caseiro, A., Fialho, P., Barata, F.,  
774 Puxbaum, H., Sanchez-Ochoa, A., Kasper-Giebl, A., Gelencser, A., Preunkert, S., Schock, M., 2007.  
775 Climatology of aerosol composition (organic versus inorganic) at nonurban sites on a west-east transect  
776 across Europe. *J. Geophys. Res.-Atmos.* 112, 1-15. <https://doi.org/10.1029/2006JD008038>.

777 Reimann, C., Caritat, P., 2000. Intrinsic flaws of element enrichment factors (EFs) in environmental  
778 geochemistry. *Environ. Sci. Technol.* 34(24), 5084–5091. <https://doi.org/10.1021/es001339o>.

779 Ricca, M., Le Pera, E., Licchelli, M., Macchia, A., Malagodi, M., Randazzo, L., Rovella, N.,  
780 Ruffolo, S.A., Weththimuni, M.L., La Russa, M.F., 2019. The CRATI Project: New Insights on the  
781 Consolidation of Salt Weathered Stone and the Case Study of San Domenico Church in Cosenza (South  
782 Calabria, Italy). *Coatings* 9, 330-345. <https://doi.org/10.3390/coatings9050330>.

783 Robaa, S.M., 2003. Urban–suburban/rural differences over Greater Cairo, Egypt. *Atmosfera* 16,  
784 157–171.

785 Robinson, A.L., Donahue, N.M., Shrivastava, M.K., Weitkamp, E.A., Sage, A.M., Grieshop, A.P.,  
786 Lane, T.E., Pierce, J.R., Pandis, S.N., 2007. Rethinking Organic Aerosols: Semivolatile Emissions and  
787 Photochemical Aging. *Science* 315(5816), 1259-1262. <https://doi.org/10.1126/science.1133061>.

788 Rodriguez-Navarro, C., Sebastian, E., 1996. Role of particulate matter from vehicle exhaust on  
789 porous building stones (limestone) sulfation. *Sci. Total Environ.* 187, 79–91. [https://doi.org/10.1016/0048-](https://doi.org/10.1016/0048-9697(96)05124-8)  
790 [9697\(96\)05124-8](https://doi.org/10.1016/0048-9697(96)05124-8).

791 Rovella, N., Aly, N., Comite, V., Ruffolo, S.A., Ricca, M., Fermo, P., Alvarez De Buergo, M., La  
792 Russa, M.F., 2020. A Methodological approach to define the state of conservation of the stone materials used  
793 in the Cairo historical heritage (Egypt). *Archaeol. Anthropol. Sci.* in press. [https://doi.org/10.1007/s12520-](https://doi.org/10.1007/s12520-020-01126-x)  
794 [020-01126-x](https://doi.org/10.1007/s12520-020-01126-x).

795 Ruffolo, S.A., Comite, V., La Russa, M.F., Belfiore, C.M., Barca, D., Bonazza, A., Crisci, G.M.,  
796 Pezzino, A., Sabbioni, C., 2015. An analysis of the black crusts from the Seville Cathedral: A challenge to  
797 deepen the understanding of the relationships among microstructure, microchemical features and pollution  
798 sources. *Sci. Total Environ.* 502, 157-166, <https://doi.org/10.1016/j.scitotenv.2014.09.023>.

799 Saarikoski, S., Timonen, H., Saarnio, K., Aurela, M., Jarvi, L., Keronen, P., Kerminen, V.M.,  
800 Hillamo, R., 2008. Sources of organic carbon in fine particulate matter in northern European urban air.  
801 *Atmos. Chem. Phys.* 8, 6281-6295. <https://doi.org/10.5194/acp-8-6281-2008>.

802 Sanjurjo Sánchez, J., Vidal Romaní, J.R., Alves, C., 2011. Deposition of particles on gypsum-rich  
803 coatings of historic buildings in urban and rural environments. *Constr. Build. Mater.* 25, 813–822.  
804 <https://doi.org/10.1016/j.conbuildmat.2010.07.001>.

805 Schauer, J.J., Kleeman, M., Cass, G., Simoneit, B.R., 1999. Measurement of emissions from air  
806 pollution sources. 1. C1 through C29 organic compounds from meat charbroiling. *Environ. Sci. Technol.*  
807 33(10), 1566–1577. <https://doi.org/10.1021/es980076j>.

808 Schauer, J.J., Kleeman, M.J., Cass, G.R., Simoneit, B.R., 2002. Measurement of emissions from air  
809 pollution sources. 5. C1-C32 organic compounds from gasoline-powered motor vehicles. *Environ. Sci.*  
810 *Technol.* 36, 1169–1180. <http://dx.doi.org/10.1021/es0108077>.

811 Shaltout, A.A., Welz, B., Castilho, I.N.B., 2013a. Determination of Sb and Mo in Cairo's dust using  
812 high resolution continuum source graphite furnace atomic absorption spectrometry and direct solid sample  
813 analysis. *Atmos. Environ.* 81, 18–24. <http://dx.doi.org/10.1016/j.atmosenv.2013.08.049>.

814 Shaltout, A.A., Khoder, M.I., El-Abssawy, A.A., Hassan, S.K., Borges, D.L.G., 2013b.  
815 Determination of rare earth elements in dust deposited on tree leaves from Greater Cairo using inductively  
816 coupled plasma mass spectrometry, *Environ. Pollut.* 178, 197–201.  
817 <http://dx.doi.org/10.1016/j.envpol.2013.03.044>.

818 Shaltout, A.A., Boman, J., Welz, B., Castilho, I.N.B., Al Ashkar, E.A., Gaita, S.M., 2014. Method  
819 development for the determination of Cd, Cu, Ni and Pb in PM<sub>2.5</sub> particles sampled in industrial and urban  
820 areas of Greater Cairo, Egypt, using high-resolution continuum source graphite furnace atomic absorption  
821 spectrometry. *Microchem. J.* 113, 4–9. <https://doi.org/10.1016/j.microc.2013.10.009>.

822 Simaõ, J., Ruiz-Agudo, E., Rodriguez-Navarro, C., 2006. Effects of particulate matter from gasoline  
823 and diesel vehicle exhaust emissions on silicate stones sulfation. *Atmos. Environ.* 40, 6905–6917.  
824 <https://doi.org/10.1016/j.atmosenv.2006.06.016>.

825 Tidblad, J., Kucera, V., Ferm, M., Kreislova, K., Brüggerhoff, S., Doytchinov, S., Screpanti, A.,  
826 Grøntoft, T., Yates, T., De La Fuente, D., Roots, O., Lombardo, T., Simon, S., Faller, M., Kwiatkowski, L.,  
827 Kobus, J., Varotsos, C., Tzanis, C., Krage, L., Schreiner, M., Melcher, M., Grancharov, I., Karmanova, N.,  
828 2012. Effects of air pollution on materials and cultural heritage: ICP materials celebrates 25 years of  
829 research. *Int. J. Corros.* 1-16. <https://doi.org/10.1155/2012/496321>.

830 Török, Á., Licha, T., Simon, K., Siegesmund, S., 2011. Urban and rural limestone weathering; the  
831 contribution of dust to black crust formation. *Environ. Earth Sci.* 63, 675–693.  
832 <https://doi.org/10.1007/s12665-010-0737-6>.

833 Vassura, I., Venturini, E., Marchetti, S., Piazzalunga, A., Bernardi, E., Fermo, P., Passarini, F., 2014.  
834 Markers and influence of open biomass burning on atmospheric particulate size and composition during a  
835 major bonfire event. *Atmos. Environ.* 82, 218–225. <https://doi.org/10.1016/j.atmosenv.2013.10.037>.

836 Wahba, M.M., Zaghoul, A.M., 2007. Adsorption characteristic of some heavy metals by some soil  
837 minerals. *Res. J. Appl. Sci.* 3(6), 421 – 426.

838 Whalley, B., Smith, B., Magee, R., 1992. Effects of particular air pollutants on materials:  
839 investigation of surface crust formation. In: Stone cleaning and the nature, soiling and decay mechanisms of  
840 stone: proceedings of the international conference held in Edinburgh, UK, 14-16 April 1992, pp. 227-234.

841 Williams, C., 2002. Islamic Monuments in Cairo: The Practical Guide. The American University in  
842 Cairo Press, Cairo.

843 Zakey, A.S., Wahab, M.A., Pettersson, J.B.C., Gatari, M.J., Hallquist, M., 2008. Seasonal and spatial  
844 variation of atmospheric particulate matter in a developing megacity, the Greater Cairo, Egypt. *Atmósfera*  
845 21(2), 171-189.

846

847

848

849

850

851

852

853

854

855

856

857

858

859

860

861

862

863

864 **Caption Figures**

865

866 Fig. 1. Microphotographs obtained by OM observations highlighting the main textural features of  
867 the limestones and the overlaying black crusts. The red dashed lines mark the contact  
868 substrate/crust. Each image is relative to a different sample at 5X magnification. a) sample 2  
869 (Crossed Polarized Light view - CPL). b) Sample 14 (Plane Polarized Light view – PPL). c) Sample  
870 15 (CPL). d) Sample E (CPL). e) Sample H (CPL).

871

872

873 Fig. 2. EFs of black crusts from Salah El Din Citadel and Magra El-Oyoun sampling sites, Qaitbay  
874 Mosque, Sultan Faraj ibn Barquq Mosque and Qansuh Al-Ghuri Mausoleum sampling sites.

875

876 Fig. 3. Box plot variations of heavy metal concentrations in black crusts samples.

877

878 Fig. 4. Graph of the OC and EC concentrations (wt.%) obtained from the analysis of the black crust  
879 samples in relation to the sampling height for each site. The monuments of the entire Cairo data set  
880 are: a) Al Manial Palace; b) Magra El-Oyoun wall; c) Salah El Din citadel; d) Tower of Bab Al  
881 Azab; e) Qaitbay Mosque; f) Sultan Faraj ibn Barquq Mosque (collection of a new sample 15), g)  
882 Quansuh Al-Ghury Mausoleum; h) Al Silahdar Mosque.

883 \* after Rovella et al. (2020).

884

885 Fig 5. a) EC vs OC binary diagram of the crust samples analysed by the different monuments in  
886 Cairo (this work and after Rovella et al., 2020); b) map of the city of Cairo where the different  
887 monuments are located.

888

889 Fig. 6. a) Binary diagram OC vs EC of the analysed black crusts. b) Histogram of the average  
890 OC/EC ratios of the analyzed black crust from the Cairo city (this work and after Rovella et al.,  
891 2020). Literature data used for the comparison refer to the crust samples taken from Cairo after  
892 Rovella et al., 2020; from the Trevi Fountain in Rome (La Russa et al., 2017); from several private  
893 buildings in Venice (La Russa et al., 2018), from the Church of Santa Maria delle Grazie in Milan  
894 (Comite and Fermo, 2018) and from the Cathedral of Monza located in the homonymous city  
895 (Comite et al., 2020).

896

897

898

899

900

901

902

**Table**[Click here to download Table: Table 1.docx](#)

**Table 1** Information about samples in terms of position and age of construction (William, 2004). They consist of both black crust and limestone substrate.

<b>Monument</b>	<b>Sample ID</b>	<b>Position</b>	<b>Height of sampling</b>
Salah El Din citadel (1176-1183)	2	Western walls	1 m
	3		1,90 m
Magra El-Oyoun (1193)	12	Western walls	2,5 m
	14		1,3 m
Sultan Faraj ibn Barquq Mosque (1400-1411)	15	Main Facade	2,5 m
Qaitbay Mosque (1472-1474)	B	Main Facade	0,80 m
	E		1,0 m
Qansuh Al-Ghuri Mausoleum (1503-1505)	H	Main Facade	1,8 m



**Table**[Click here to download Table: Table 2.docx](#)**Table 2** TC (Total Carbon), OC (Organic Carbon), EC (Elemental Carbon) OX (Oxalate) CC (Carbonate Carbon) Gy (Gypsum) concentrations (wt%); and OC/EC and EC/TC ratio

<b>Sample</b>	<b>TC</b>	<b>OC</b>	<b>EC</b>	<b>OX</b>	<b>CC</b>	<b>Gy</b>	<b>OC/EC</b>	<b>EC/TC</b>
<b>2</b>	7.4	0.87	2.83	0.28	3.70	8.45	0.31	0.38
<b>3</b>	6.61	1.22	1.53	0.14	3.72	22.63	0.75	0.23
<b>14</b>	6.65	0.96	2.40	0.15	3.14	25.55	0.40	0.36
<b>12</b>	5.43	0.75	1.45	0.22	3.01	51.25	0.52	
<b>15</b>	5.11	0.66	1.23	0.11	3.11	15.01	0.54	0.24
<b>B</b>	7.88	0.99	1.48	1.15	4.26	32.98	0.23	0.19
<b>E</b>	6.41	1.36	2.15	0.15	2.75	9.57	0.49	0.34
<b>H</b>	7.75	1.12	1.99	0.09	4.55	9.57	0.25	0.26

Figure  
[Click here to download high resolution image](#)

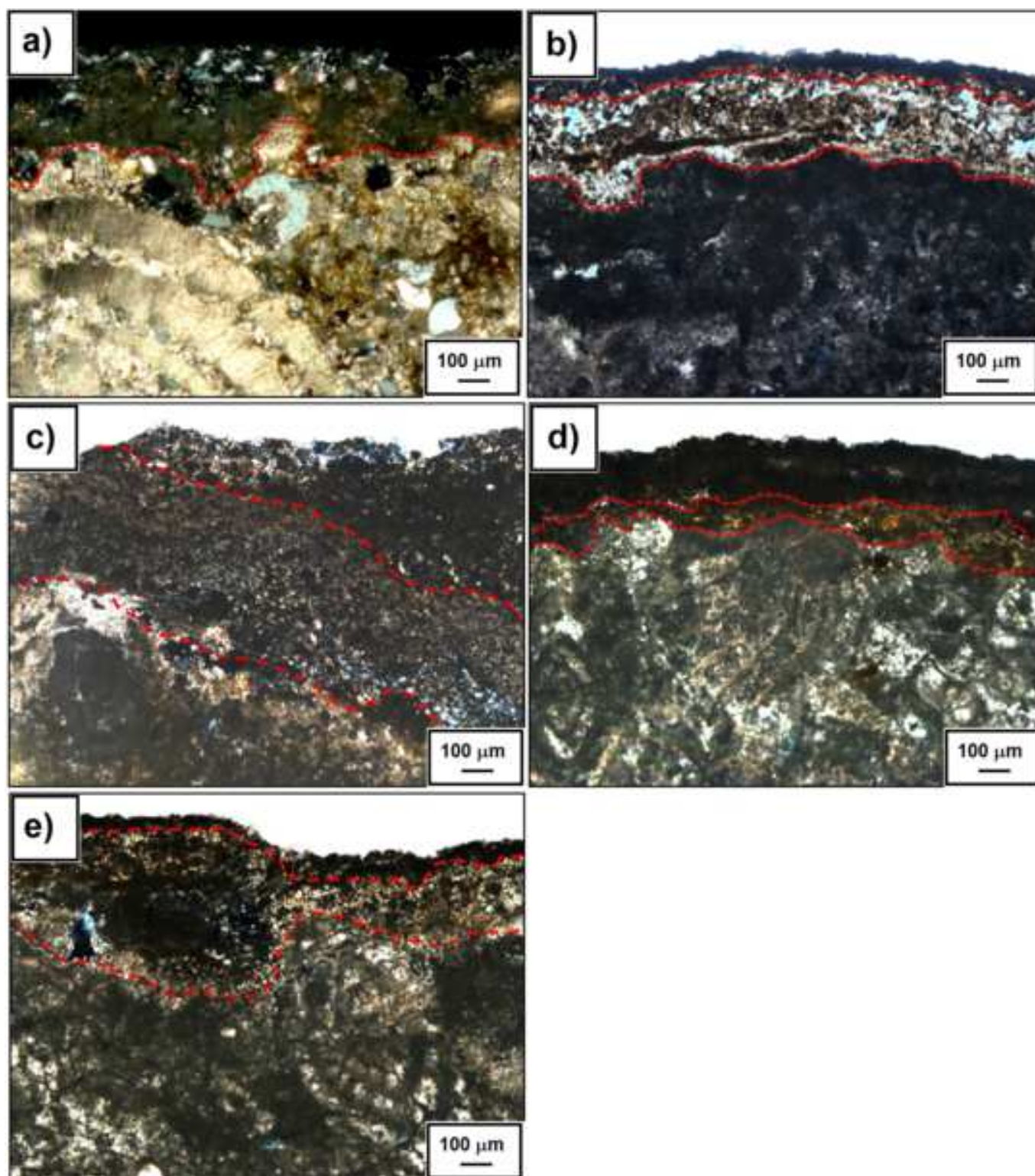


**Figure**  
[Click here to download high resolution image](#)

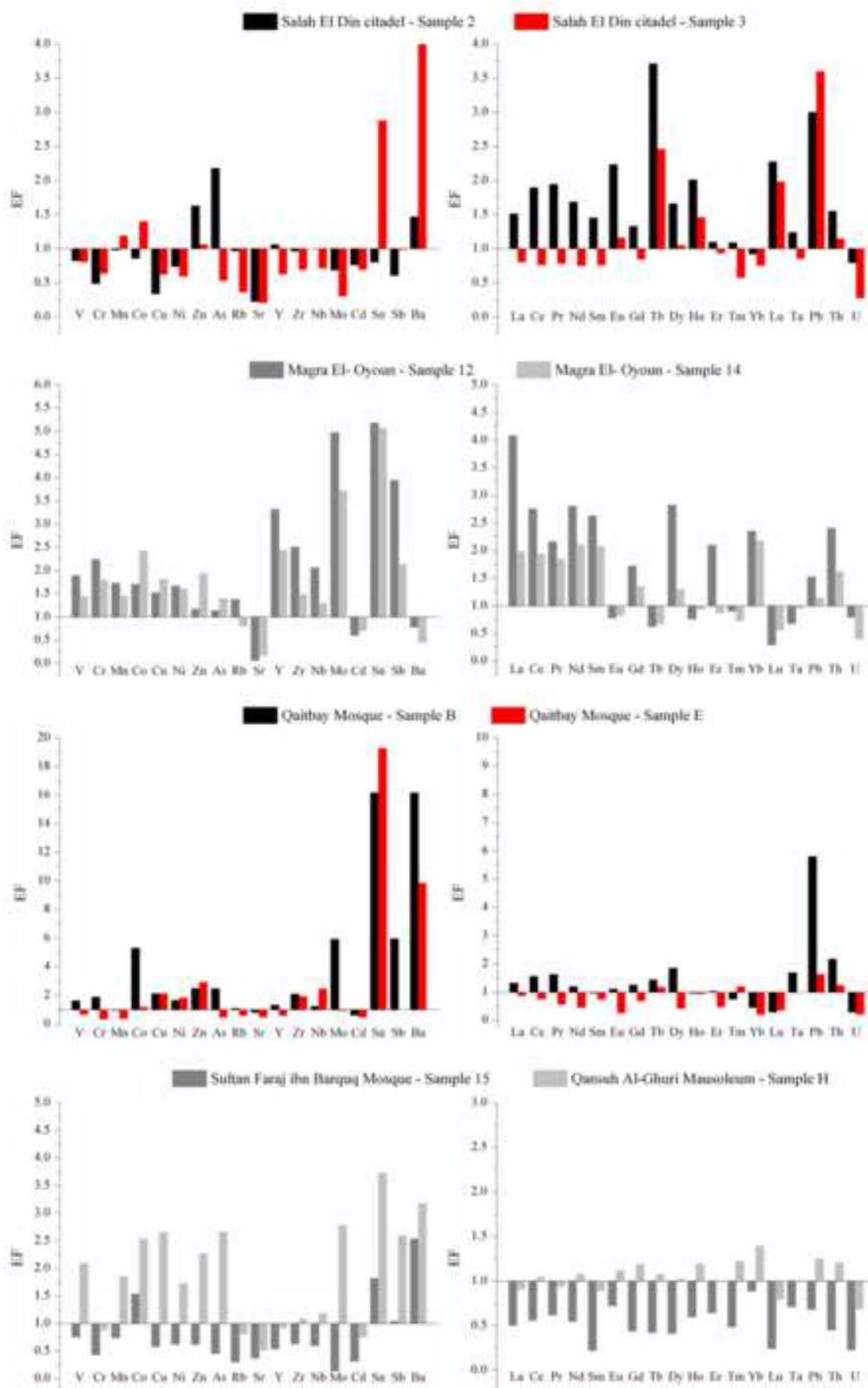


Figure  
[Click here to download high resolution image](#)

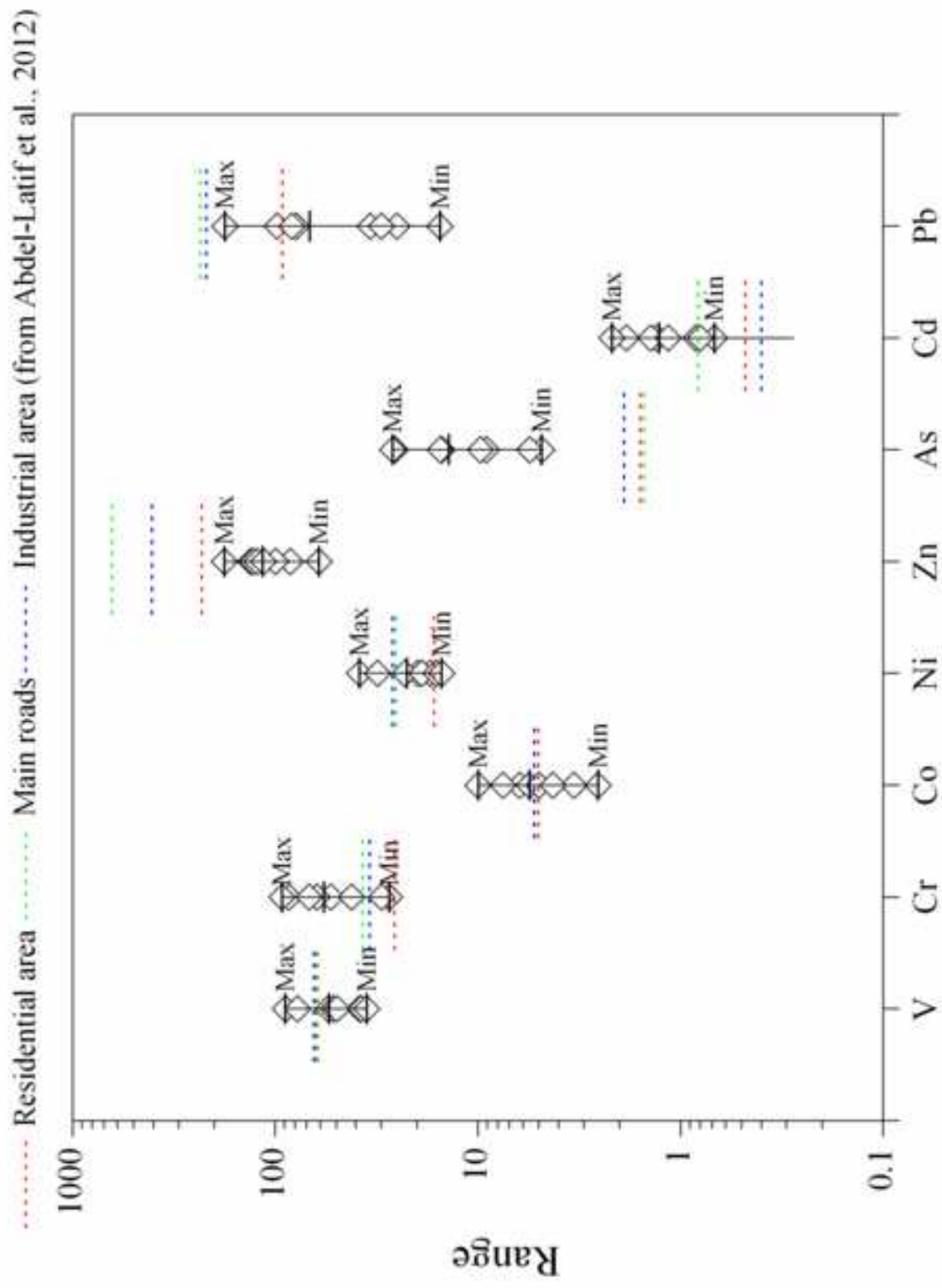
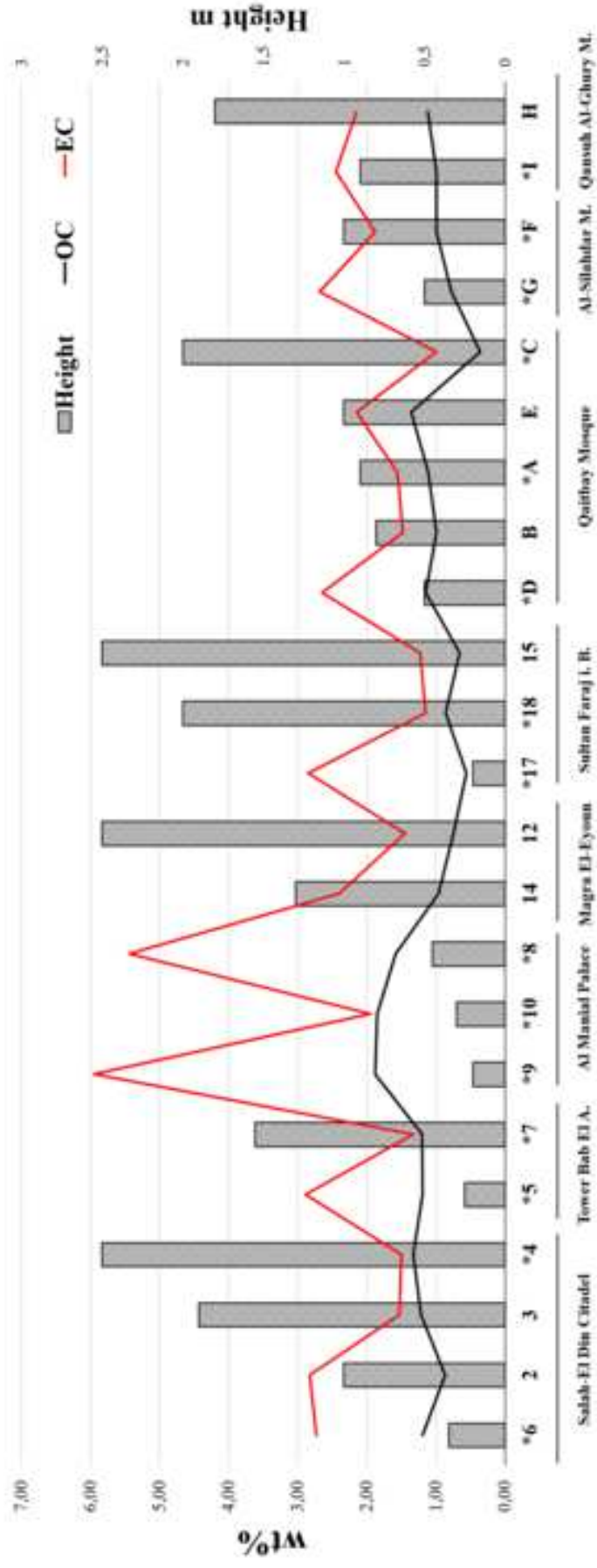


Figure  
[Click here to download high resolution image](#)



Al-Silahlidar M. Qasab Al-Ghury M.

Figure  
[Click here to download high resolution image](#)

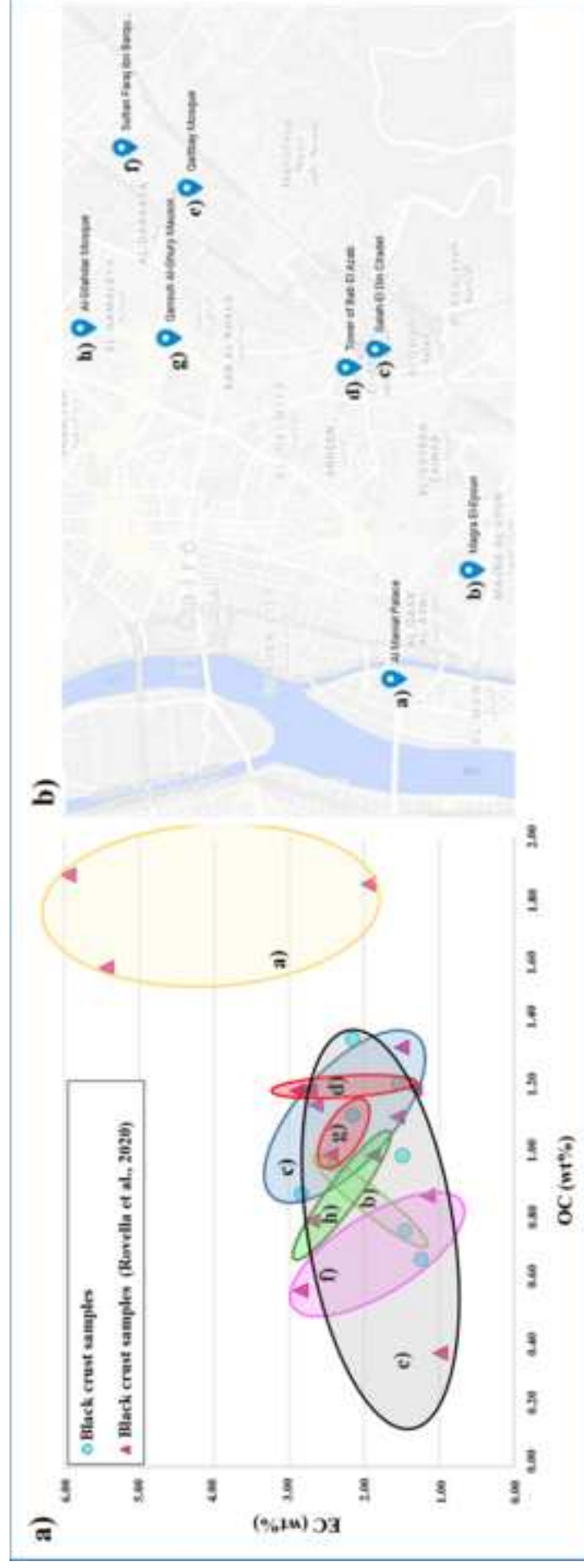
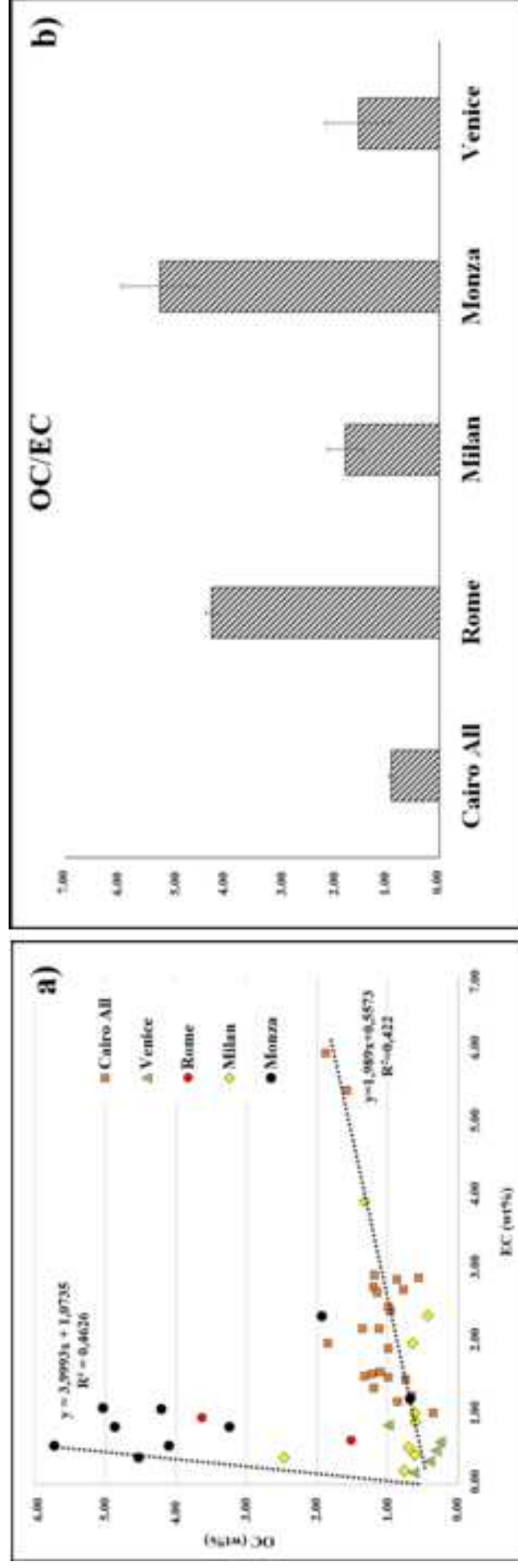


Figure  
[Click here to download high resolution image](#)



**Supplementary material for on-line publication only**

[Click here to download Supplementary material for on-line publication only: Supplementary material.pptx](#)